

Review

Kinetics of liquid-phase hydrogenation reactions over supported metal catalysts — a review

Utpal K. Singh, M. Albert Vannice*

Department of Chemical Engineering, Pennsylvania State University, 158 Fenske Lab, University Park, PA 16802, USA

Received 29 June 2000; received in revised form 3 November 2000; accepted 4 November 2000

Abstract

The kinetics of liquid-phase hydrogenation reactions have been reviewed with a special emphasis on α , β -unsaturated aldehydes as reactants. These reactions can be complex and can be influenced by factors such as metal specificity, side reactions, and metal-support interactions as well as reaction parameters. The importance of results in the absence of heat and mass transfer limitations has been emphasized. Hydrogenation reactions are typically assumed to be structure-sensitive, but dependencies on metal crystallite size have been reported; however, this behavior has been attributed to side reactions which can inhibit activity. Finally, solvent effects can exist, but the effect of H_2 concentration in the liquid phase has infrequently been isolated. Thermodynamic arguments indicate that a solvent effect can enhance the surface coverage of hydrogen on the catalyst surface at a constant H_2 partial pressure, but in the absence of any solvent effects, surface coverage is independent of the liquid-phase H_2 concentration. © 2001 Elsevier Science B.V. All rights reserved.

Keywords: Hydrogenation; Aldehydes; Group VIII metals; Structure sensitivity; Mass transfer

1. Introduction

The application of catalytic techniques for the production of fine chemicals and pharmaceuticals is important, especially with increased environmental awareness. Table 1 displays order of magnitude estimates for the quantity of by-products formed per kg of product, termed the *E*-factor [1]. An *E*-factor of 1–5 is common in the bulk and commodity chemicals industry, and some petrochemical processes can exhibit values as low as 0.1. In contrast, significantly higher *E*-factors are encountered in the specialty chemical and pharmaceutical sectors where values as high as

50–100 can be obtained. Such a large *E*-factor has been attributed, at least in part, to multi-step syntheses using stoichiometric reagents that result in accumulation of inorganic salts that need to be removed from the final product. Admittedly, the use of the *E*-factor alone is a gross oversimplification, nevertheless, these values highlight the need for development of selective catalytic routes for transformations relevant in fine chemicals and pharmaceuticals. Significant efforts are focused on development of homogeneous catalytic techniques that offer significant potential because they can be molecularly tuned through ligand modification. Molecular tuning of heterogeneous catalysts is more difficult; however, such catalysts have enormous advantages compared to their homogeneous counterparts in terms of ease of handling, separation,

* Corresponding author.
E-mail address: mavche@engr.psu.edu (M.A. Vannice).

Table 1
E-factors for various sectors of the chemical industry [1]

Industry sector	Amount of product (t)	E-factor (kg by-product/kg product)
Bulk chemicals	10^4 – 10^6	<1–5
Fine chemicals	10^2 – 10^4	5–50
Pharmaceuticals	10 – 10^3	25–100

catalyst recovery, and regeneration that make them industrially attractive.

Hydrogenation reactions are a class of reactions that are valuable in the pharmaceutical and specialty chemical industry [2–6]. A review of heterogeneously catalyzed liquid-phase hydrogenation reactions appears to be a daunting task; however, the focus of this review will be restricted to the kinetics of such reactions with a primary emphasis on hydrogenation of α,β -unsaturated aldehydes over supported metal catalysts. A survey of the literature regarding liquid-phase hydrogenation reactions reveals that much of the work performed in this area has been aimed at studying selectivity issues and only scant quantitative kinetic data are reported. This is very apparent for liquid-phase hydrogenation of α,β -unsaturated aldehydes, a field of chemistry which has been extensively studied for over a decade, but only recently has had quantitative kinetics determined. These results with Pt/SiO₂ showed an unusual effect of temperature on reaction rate and product distribution [7,8]. Augustine reviewed heterogeneously catalyzed hydrogenation reactions from a selectivity standpoint and outlined a number of different hydrogenation reactions; however, reaction kinetics were not addressed [9]. A kinetic approach to a better mechanistic understanding of liquid-phase hydrogenation reactions has already proven to be valuable [7,8,10–12], and the discussion that follows will highlight some of the important aspects describing the kinetic behavior of liquid-phase hydrogenation reactions.

2. Mass (and heat) transfer effects

A critical step in obtaining reliable quantitative kinetics is to ensure the absence of all transport limitations including external and internal heat and mass transfer effects as well as the rate of hydrogen transfer from the gas phase to the liquid phase. In gen-

eral, temperature gradients arising from heat transfer limitations are not as prevalent under liquid-phase reaction conditions compared to the vapor phase because heat capacities and thermal conductivities of the liquid phase are an order of magnitude higher compared to the gas phase. Numerous texts have addressed transport limitations for reactions in porous catalysts [13,14]; therefore, the discussion here will be limited to summarizing criteria to show whether transport limitations are absent and to describing ways in which mass transfer effects can alter reaction kinetics in the liquid phase.

One of the most definitive criteria for evaluation of the significance of transport limitations with supported metal catalysts is the Madon–Boudart test, which is a variation of the Koros–Novak criterion [15,16]. Application of a method to ascertain the presence or absence of transport limitations should be considered mandatory prior to obtaining reaction kinetics using supported metal catalysts. The Madon–Boudart test utilizes the fact that in the absence of all transport limitations, the rate of a reaction is proportional to the number of active sites. For reactions on supported metal catalysts, this test requires the preparation of at least two catalysts with widely varying concentrations of surface metal atoms. If the reaction is structure insensitive the active site density will be proportional to the number of surface metal atoms, which can be measured by various chemisorption methods. If the reaction is, or may be, structure sensitive then metal dispersion (the ratio of surface metal atoms, M_s , to the total number of metal atoms, M_t) must be kept constant or similar among the catalysts. In the absence of transport limitations, a ln–ln plot of the activity versus the surface metal atom concentration will exhibit a linear correlation with a slope of unity. Control by internal (pore) diffusion gives a slope of 0.5 while external diffusion control gives a slope of zero [15]. When this test is performed at two or more reaction temperatures, it can verify that both heat

and mass transfer effects are absent. Another way that this can be stated is that in the absence of any transport limitations, the turnover frequency (TOF, molecule/s/ M_s) for catalysts with widely varying concentrations of surface metal atoms but similar dispersions should be the same. One of the advantages of the Madon–Boudart test is that it is applicable to any rate expression and is not limited to simple power law rate expressions. A variation of the Madon–Boudart test has been proposed, but it suffers from the fact that it requires poisoning the catalyst with CS_2 ; thus problems exist because of chromatographic effects and the alteration of surface structure due to S adsorption, which can modify the reaction kinetics [17].

The Madon–Boudart test was utilized by Singh and Vannice in their study of citral hydrogenation over SiO_2 - and TiO_2 -supported Group VIII metals [7,12,18]. Fig. 1 displays a plot of $\ln(\text{activity})$ versus $\ln(\text{Pd surface concentration})$ for this reaction over SiO_2 - and $\eta\text{-}Al_2O_3$ -supported Pd catalysts at 300 K and atmospheric pressure [18]. A slope of unity indicated that all mass transport limitations and poisoning effects are absent from the kinetic data and the use of the Weisz criterion [19] also showed the absence of mass transfer effects. Since Pd/ SiO_2 was the most active of all the SiO_2 -supported Group VIII metals studied for citral hydrogenation, the application of the Madon–Boudart test to Pd was sufficient to verify the absence of transport limitations with all the other SiO_2 -supported Group VIII metals [18]. This test was

also successfully applied to catalysts in which the rate of citral hydrogenation is strongly affected by Pt crystallite size as well as to complex TiO_2 -supported Pt catalysts where metal–support interactions are known to occur [7,12]. In each case a \ln – \ln plot of activity versus Pt_s concentration yielded a slope of unity, which indicated the absence of mass transfer limitations.

The absence of mass transfer limitations typically has been probed by varying the stirring speed and/or the catalyst particle size, with both approaches having limitations that have been addressed by Boudart and co-workers. The stirring speed test checks the mass transfer resistance of H_2 from the gas phase to the bulk liquid phase and the reactant transport from the bulk liquid phase to the catalyst surface, and the absence of external mass transfer limitations requires that the impeller speed be increased till the reaction rate remains constant with stirring speed. However, Chambers and Boudart have shown that some laboratory scale reactors operate at such low particle Reynolds numbers that mass transfer coefficients are insensitive to flow rate changes; thus, even if the rate is invariant to the stirring rate, mass transfer limitations may still exist [20]. The particle size test is used to check for the significance of internal diffusion resistance, and smaller catalyst particles are used in an effort to eliminate internal diffusion resistance. Boudart has pointed out how this test loses significance if a bimodal pore distribution exists because the absence of a rate change with decreasing particle size can indicate the absence of diffusion limitations within the large pores of the catalyst, but diffusion limitations may still be significant in the smaller pores. The Weisz–Prater criterion can also be used to verify the absence of internal diffusion limitations. The advantage of this criterion is that it offers a test utilizing values that can be directly measured or calculated. The Weisz–Prater parameter is a dimensionless number representing the ratio of the reaction rate to the rate of internal diffusion. The absence of significant internal diffusion limitations is verified if the value of this dimensionless parameter is less than 0.3 for reaction orders of 2 and lower order [19]. Finally, the significance of mass transfer effects can also be checked using the Thiele modulus, which provides an effectiveness factor representing the ratio of the actual reaction rate to that occurring in the absence of our

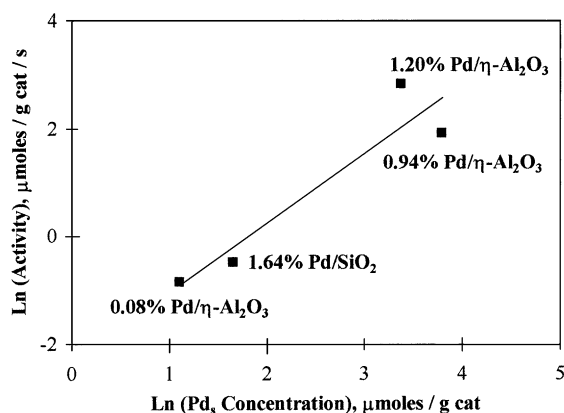


Fig. 1. Madon–Boudart test for citral hydrogenation on SiO_2 - and $\eta\text{-}Al_2O_3$ -supported Pd catalysts at 300 K, 1 atm H_2 and 0.06 M citral in hexane (from [18]).

diffusional constraints [21]. In general, large values of the Thiele modulus indicate the presence of diffusion limitations, while small values indicate the absence of diffusion limitations. Utilization of the Thiele moduli and effectiveness factors requires some knowledge of catalyst geometry and the reaction orders.

Mass transfer effects can have a pronounced effect on reaction kinetics. Roberts and Lam studied the effect of pore diffusion resistance on a reaction network consisting of a slow irreversible reaction occurring in parallel with a fast reversible reaction. They reported that the apparent activation energy in the presence of pore diffusion limitations is not always 1/2 of the intrinsic activation energy [22], as is the case for a simple n th-order reaction. Instead, they showed that, depending on the equilibrium constant and the heat of reaction for the fast reversible reaction, the observed activation energy is negative for an endothermic reaction and can be much greater than the intrinsic activation energy for an exothermic reaction [22]. The result would have been even more complex if Langmuir–Hinshelwood kinetics were used in place of the first-order rate law. Some researchers have explicitly included transport limitations in their kinetic model to describe the liquid-phase hydrogenation of various aromatics [23–26]; however, no selectivity comparisons were made and, therefore, it is not clear whether transport limitations affected their product distributions.

In a series of papers examining enantioselective liquid-phase hydrogenation of ethyl pyruvate to R - and S -ethyl lactate over cinchonidine-modified Pt/Al₂O₃ catalysts, Blackmond and co-workers clearly showed that product distribution was altered by bulk diffusion limitations, i.e. the transport of H₂ from the gas phase to the liquid phase [27–30]. Fig. 2 shows the enantiomeric excess (defined as the ratio of the difference between the concentrations of R - and S -enantiomers to their sum) for ethyl pyruvate hydrogenation at various stirring speeds. It is apparent that a bulk mass transfer limitation suppressed production of the R -enantiomer. There was also a pronounced pressure effect, and the enantiomeric excess (ee) for the R -enantiomer increased as the H₂ pressure increased from 1 to 40 atm. Blaser and co-workers attributed this behavior to a difference in the rate determining step for the formation of the two enantiomers, i.e. addition of the first H atom as the rate determining step (RDS) for

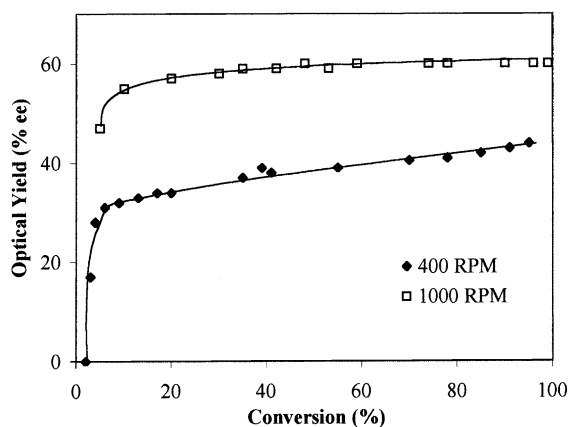


Fig. 2. Effect of stirring speed on enantiomeric excess (defined in text) during enantioselective hydrogenation of ethyl pyruvate over cinchonidine modified Pt/Al₂O₃ (from [27]).

the S -enantiomer compared to addition of the second H atom as the RDS for the R -enantiomer [31]. Blackmond and co-workers, on the other hand, have rationalized the pressure effect on the basis of a kinetic coupling of the two pathways for formation of the R - and S -enantiomers. They developed a kinetic model invoking the steady-state approximation to determine the surface concentration of ethyl pyruvate adsorbed on the modified sites. At low H₂ pressures, their model collapsed to the case of quasi-equilibrium for adsorption of pyruvate and irreversible addition of adsorbed H to the adsorbed pyruvate. At high H₂ pressures, the RDS shifted to pyruvate adsorption on the modified sites. At intermediate hydrogen pressures, the relative rates of formation of the R - and S -enantiomers varied with pressure due to differing sensitivities of each rate on H₂ pressure, as determined by the rate constants in the respective pathways [29,32].

The product distribution when bulk mass transfer limitations were present was correlated with the maximum rate of H₂ transfer from the gas phase to the liquid phase, which can be defined as follows:

$$r_{\max}^{\text{H}_2} = k_L a [\text{H}_2]_{\text{sat}} \quad (1)$$

where $k_L a$ and $[\text{H}_2]_{\text{sat}}$ are the mass transfer coefficient and the equilibrium concentration of H₂ in the liquid phase, respectively. The rate of H₂ transport from the gas phase to the liquid phase is, in general, the product of $k_L a$ and the difference between the H₂

concentration in the liquid phase and its equilibrium concentration, i.e. $[H_2] - [H_2]_{\text{sat}}$; hence the maximum rate of H_2 transport is obtained when the concentration of H_2 in solution is negligible. The mass transfer coefficient for H_2 transfer from the gas phase to the liquid phase was determined using the procedure of Deimling et al. [33], which involves degassing the liquid with a N_2 purge prior to introducing H_2 and commencing agitation [27,33]. H_2 was introduced into the reactor, which was maintained at constant temperature and pressure, from a reservoir that was initially at a pressure P_i . The rate of H_2 uptake was monitored by the pressure decay in the reservoir after the impeller was started, and the mass transfer coefficient ($k_L a$) and H_2 solubility were determined using the following equation [33]:

$$\frac{P_f - P_0}{P_i - P_0} \ln \left(\frac{P_i - P_f}{P - P_f} \right) = k_L a t \quad (2)$$

where P_f , P_0 , P_i , and P , are the final reservoir pressure after equilibration, the solvent vapor pressure, the initial reservoir pressure prior to start of agitation, and the system pressure, respectively, and t is the time. Assuming the vapor pressure of the solvent to be negligible compared to the total system pressure, a plot of $(P_f/P_i) \ln[(P_i - P_f)/(P - P_f)]$ versus time is linear with a slope equal to $k_L a$. The equilibrium H_2 solubility can also be obtained with this procedure by using the difference in H_2 pressure between the final and initial stages and assuming the ideal gas law to be valid for the gas phase [33]. Fig. 3 summarizes the results of Sun et al. regarding the influence of bulk mass transfer resistance on the product distribution during ethyl pyruvate hydrogenation at 303 K. The stirring speed was varied from 400 to 2000 rpm at 5.7 atm to change $k_L a$ and to increase r_{max} by more than two orders of magnitude from 0.0035 mol/l/min at the lower speed to 0.507 mol/l/min at the higher speed. This resulted in a change in ee from 24 to 60% at a conversion of 50%. The results indicate a sharp rise in the ee upon increasing the stirring speed from 400 to 750 rpm; however, little change was detected upon a further increase in the stirring rate from 750 to 2000 rpm because the rate of H_2 transport is no longer rate controlling and the reaction occurs in the kinetic regime. The maximum rate of H_2 transport from the gas phase to the liquid phase could be altered either by varying the stirring speed at a constant pressure, which affects

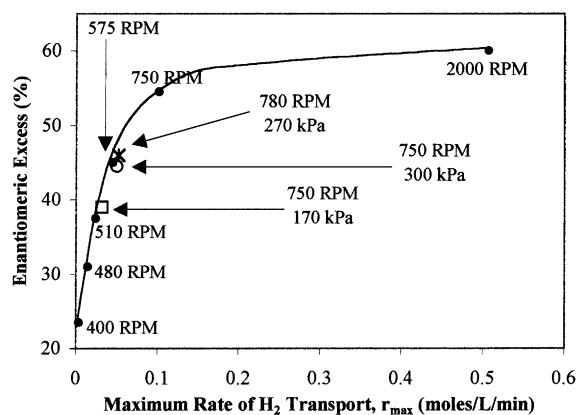


Fig. 3. Correlation of enantiomeric excess with the maximum rate of hydrogen delivery (defined in text) during ethyl pyruvate hydrogenation over a cinchonidine modified Pt/Al_2O_3 catalyst (from [28]).

$k_L a$, or by changing the H_2 pressure at a constant stirring speed, which in turn changes the equilibrium concentration of H_2 in the liquid phase. Performing the reaction at different H_2 pressures, i.e. 1.70, 2.66, and 3.00 atm, but at the same stirring speed of 750 rpm duplicated the trend in product distribution which occurred as the stirring speed varied at constant pressure (open square, open circle, and star in Fig. 3) [28].

The effect of transport limitations on product distribution for liquid-phase reactions has also been shown for the hydrogenation of fatty oils over Ni [34] where monounsaturated acids were desired rather than the completely saturated product. High selectivities to the former were obtained under a H_2 transfer-limited regime, i.e. the rate of H_2 transfer from the gas phase to the liquid phase was the slow step. Such conditions were obtained by operating at low pressures with slow stirring rates.

The examples just discussed demonstrate that extra precautions must be taken to ensure the absence of all transport limitations prior to the evaluation of accurate reaction kinetics. Sun et al. have shown that variations in product distribution between different studies at seemingly identical conditions can be due to mass transfer effects [28], which further reinforces the need to verify the absence of all transport limitations prior to obtaining kinetic data. The most versatile test for evaluating the significance of transport resistances on supported-metal catalysts is the Madon–Boudart test because it can check for external and internal heat and

mass transfer limitations along with bulk mass transfer limitations for any type of reaction [15].

3. Solvent effects

Solvent effects are well documented in the organic synthesis literature [35]. Similar effects have also been reported in the heterogeneous catalysis literature; however, the mechanistic basis of the observed effects is not clear. Solvent effects in heterogeneous catalysis have been rationalized by correlating reaction rates and product distributions with solvent polarity or dielectric constant [36–39]. While there is no doubt that such solvent properties can influence reaction kinetics, much work remains to be done to better understand and quantitatively characterize these effects, which are even more complicated with supported metal catalysts due to possible interactions between the solvent and the support [40–42].

Solvent effects can influence the kinetics of competitive hydrogenation reactions of both polar and non-polar substrates. It has been found that a polar solvent enhances adsorption of the non-polar reactant while a non-polar solvent enhances the adsorption of a polar reactant. For example, competitive hydrogenation of acetone and cyclohexene in a polar solvent enhanced adsorption and reaction of cyclohexene, presumably due to strong interactions between the polar solvent and acetone in the bulk fluid phase resulting in reduced affinity for acetone adsorption. In contrast, competitive hydrogenation in a non-polar solvent enhanced adsorption and reaction of acetone [41–43]. Interaction of reactants in the bulk fluid phase can affect reaction kinetics on heterogeneous catalysts. Rajadhyaksha and Karwa studied liquid-phase hydrogenation of *o*-nitrotoluene over Pd/carbon at 333 K and 14 atm and were able to correlate their reaction rates with activity coefficients, which are a measure of non-ideal interactions in the fluid phase. In addition, they showed that this correlation also held for Lemcoff's results for liquid-phase acetone hydrogenation over Raney nickel in various solvents [44,45]. Data extracted from the results of Cerveny et al. are shown in Fig. 4 for the competitive hydrogenation of 1-hexene and 2-methyl-3-buten-2-ol over SiO₂-supported Pt in various polar and non-polar solvents [43]. The authors have chosen a rather un-

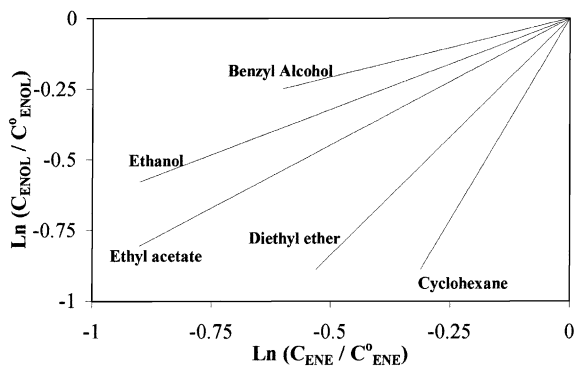


Fig. 4. Solvent effect during competitive hydrogenation of 2-methyl-3-buten-2-ol (ENOL) and 1-hexene (ENE) over Pt/SiO₂ (from [42]).

conventional method for representing their data, but as the following discussion will show, their results are in agreement with the qualitative explanation just presented. Using a conventional Langmuir–Hinshelwood type rate expression, assuming dissociative adsorption of hydrogen and choosing addition of the second H atom as the RDS, the ratio of the rates of disappearance of 2-methyl-3-buten-2-ol (ENOL) and cyclohexene (ENE) can be expressed as

$$\frac{r_{\text{ENOL}}}{r_{\text{ENE}}} = \frac{k_{\text{ENOL}} K_{\text{ENOL}} C_{\text{ENOL}}}{k_{\text{ENE}} K_{\text{ENE}} C_{\text{ENE}}} \quad (3)$$

where k_i , K_i , and C_i , are the rate constant, adsorption equilibrium constant, and bulk concentration of species i , respectively. Integration of the above expression yields the following:

$$\ln \left(\frac{C_{\text{ENOL}}}{C_{\text{ENOL}}^0} \right) = \frac{k_{\text{ENOL}} K_{\text{ENOL}}}{k_{\text{ENE}} K_{\text{ENE}}} \ln \left(\frac{C_{\text{ENE}}}{C_{\text{ENE}}^0} \right) \quad (4)$$

where C_i^0 and C_i are the initial concentration of species i and at time t , respectively. A plot of $\ln(C_{\text{ENOL}}/C_{\text{ENOL}}^0)$ versus $\ln(C_{\text{ENE}}/C_{\text{ENE}}^0)$ yields the ratio of the apparent rate constants for two substrates during competitive hydrogenation, and the larger the slope the greater the relative reactivity of the non-polar substrate (ENOL) while the smaller the slope the greater the relative reactivity of the non-polar substrate (ENE). Consistent with the previous statements, Fig. 4 shows that cyclohexane (a non-polar solvent) provides the largest slope and hence a greater relative reactivity for the polar substrate. Furthermore, benzyl

alcohol, a polar solvent, produces the smallest slope and hence favors reactivity of the non-polar substrate. Lo and Paulaitis reinforced these ideas by showing a correlation between the competitive hydrogenation rates of acetone and cyclohexene in various solvents and the activity coefficients estimated by the UNIFAC group contribution method [46]. As an extension of these statements, solvent effects did not appreciably affect the kinetics during competitive hydrogenation of chemically similar compounds such as 1-hexene and cyclohexene [43]. The simplified approach presented above has severe limitations because the authors assumed an identical rate expression for each reactant with all the solvents they studied. Gamez et al. studied solvent effects on the kinetics of liquid-phase ethyl pyruvate hydrogenation, and their results suggested that such effects affect the binding strength of reactants, hence altering the adsorption equilibrium constants, and affecting the apparent reaction orders with respect to the reactants [47]. In addition, the analysis of Cervený and co-workers does not account for solvent chemisorption and its interaction with the surface [43]. Finally, verification of solvent effects can be further complicated by solvent decomposition, especially with alcoholic solvents [48]; consequently, more detailed kinetic studies are necessary to confirm the generalities of the hypothesis discussed previously.

Scholten and co-workers studied the vapor- and liquid-phase hydrogenation of benzene to cyclohexene on Ru in the presence of a polar modifier, which represents another mechanism by which solvent effects can modify the kinetics of liquid-phase hydrogenation reactions [49–52]. The authors noted that addition of

a polar reagent such as ethanol significantly enhanced the selectivity to cyclohexene due to its enhanced desorption rate and suppressed hydrogenation rate. The enhancement of cyclohexene desorption was attributed to a reduction in the chemisorption bond strength due to an adsorbate–adsorbate interaction between the alcohol and chemisorbed cyclohexene [49]. This was further investigated by studying vapor-phase benzene hydrogenation in the presence of an alcohol and using FTIR to characterize the alcohol–olefin interaction [52]. The formation of the adduct via hydrogen bonding of the hydroxyl group in the modifier with the C=C bond was shown to occur [53] and, as a result, it was suggested that the cyclohexene adsorption strength was weakened because the overlap of the π -electrons of the olefin with Ru was diminished, thus enhancing cyclohexene desorption. This study was performed using hexane and low alcohol concentrations, but it is not difficult to imagine that a similar mechanism might also hold true if the alcohol were used as the solvent. Further study is required in this regard. Solvent effects can also be manifested via competitive adsorption between the solvent and the reactant, and Augustine and Techasauvapak have used a single turnover reaction sequence to evaluate the importance of competitive solvent adsorption [40].

In the absence of transport limitations, apparent solvent effects can be attributed to variations in H_2 solubility in the liquid phase in some cases. Boudart and co-workers studied liquid-phase cyclohexene hydrogenation on supported Pt, Pd, and Rh crystallites in various solvents [54–56], and their results are summarized in Table 2. The TOF for cyclohexene

Table 2
Effect of H_2 solubility on liquid-phase hydrogenation of cyclohexene over SiO_2 -supported Pt, Pd, and Rh catalysts [53–55]

Solvent	H_2 solubility $\times 10^6$ (mol/cm ³) ^a	TOF for Pt/ SiO_2 ^a (s ⁻¹)	Rate constant, k , for Pt/ SiO_2 ^{a,b}	TOF for Pd/ SiO_2 ^c (s ⁻¹)	TOF for Rh/ SiO_2 ^d (s ⁻¹)	Rate constant, k , for Rh/ SiO_2 ^{b,d}
Cyclohexane	3.97	8.67	3.63	7.80	13.70	5.59
<i>n</i> -Heptane	4.85	12.57	4.30	7.98	20.00	6.59
<i>p</i> -Dioxane	1.90	4.84	4.23	–	–	–
Ethyl acetate	3.77	10.15	4.47	7.93	12.60	6.53
Methanol	3.40	7.92	3.87	7.85	14.60	6.13
Benzene	3.07	6.86	3.71	0.58 (2.78)	–	–
Cyclohexene	3.57	8.40	3.91	–	–	–

^a [55].

^b Obtained assuming H_2 dissociation is the rate determining step.

^c [53].

^d [54].

hydrogenation over Pt and Rh varied significantly in different solvents, but the TOF over Pd was independent of solvent. While the TOF for cyclohexene hydrogenation over Pt varied nearly three-fold, the rate constant based on H_2 concentration in the liquid phase was nearly constant and nearly independent of solvent. Madon et al. explained the solvent effects with Pt, in the absence of all transport limitations, by postulating that H_2 in the gas phase, the liquid phase, and the transition state just prior to adsorption were in quasi-equilibrium. The RDS was proposed to be dissociative adsorption of hydrogen and the following rate expression was obtained:

$$r = k_{\text{app}} \left(\frac{H_{H_2}}{H_T} \right) C_{H_2} \quad (5)$$

where k_{app} , H_{H_2} , H_T and C_{H_2} are the apparent solvent-independent rate constant, the Henry's law constant for H_2 in the solvent, the Henry's law constant for the transition state, and the concentration of hydrogen in the liquid phase, respectively. The above equation is similar to the classical expression for reaction rates in a thermodynamically non-ideal system as shown by Bronsted [57] and reiterated first by Wong and Eckert [58] and then by Lo and Paulaitis [46]. The influence of H_2 solubility on the rate of cyclohexene hydrogenation over Pt/SiO₂ was rationalized on the basis of the transition state resembling the parent H_2 molecule due to weak interactions of the transition state with the surface thus implying that $H_{H_2} = H_T$ and hence the rate = kC_{H_2} , where k is the solvent-independent rate constant. In this case the reaction rate is proportional to the concentration of hydrogen in the liquid phase in the absence of transport limitations. In contrast, if the transition state were interacting strongly with the surface, then H_{H_2} would not be equal to H_T and substitution of Henry's law into the above equation shows that the rate = $(k/H_T)P_{H_2}$, where k/H_T is independent of solvent. The rate is then constant at a given partial pressure of hydrogen independent of the H_2 solubility [56]. Similar behavior was observed by Boudart and Sajkowski during cyclohexene hydrogenation on Rh [55]; however, Gonzo and Boudart found that the TOF for cyclohexene hydrogenation over Pd was independent of solvent [54]. In addition, the latter authors observed a half-order dependency on hydrogen pressure during reaction over Pd compared to the first-order

dependency observed with Pt and Rh [53–55]. Both the absence of a solvent effect and the half-order dependency with respect to hydrogen pressure during cyclohexene hydrogenation over Pd was attributed to gas-phase, liquid-phase, and adsorbed hydrogen being quasi-equilibrated [59]. This argument is not completely satisfying because cyclohexene hydrogenation over all three catalysts was described by reaction of an adsorbed species that was quasi-equilibrated with hydrogen in the gas phase yet solvent effects were present with Pt and Rh but absent with Pd. With Pt and Rh, the reactive species in the RDS was the H_2 transition state for dissociative adsorption, which was equilibrated with gas-phase H_2 , whereas with Pd two reactive species were present, i.e. an adsorbed hydrogen atom and a half-hydrogenated species, both of which were quasi-equilibrated with H_2 in the gas phase and cyclohexene in the liquid phase [59]. A close inspection of the kinetic analysis in the study by Gonzo and Boudart shows that it is incomplete and the derivation of the reported rate expression based on the assumption of only one type of site is not possible; however, the assumptions of another type of site capable of adsorbing only hydrogen plus the addition of the first H atom as the RDS provides a rate expression consistent with the data.

The analysis of an analogous problem by Singh and Vannice suggests that solvent effects can also occur if quasi-equilibrium is assumed for the dissociative adsorption step for H_2 [60]. Singh and Vannice assumed that H_2 in the gas phase, the liquid phase, and the adsorbed state were in quasi-equilibrium, and they then asked whether solvent effects can alter the surface coverage of hydrogen at a constant partial pressure of hydrogen in the gas phase. A Langmuirian approach was taken to describe adsorption, i.e. no interaction between adsorbed species was assumed. Through proper choice of the standard state and the assumption that solvent adsorption was negligible, the surface coverage of hydrogen was represented as

$$\Theta_{HS} = \frac{\alpha K_H^{1/2} P_{H_2}^{1/2}}{1 + \alpha K_H^{1/2} P_{H_2}^{1/2}} \quad (6)$$

where K_H is the solvent-independent adsorption equilibrium constant for dissociatively adsorbed H_2 , and α is a measure of the non-ideality imposed by the solvent, which is defined as follows:

$$\alpha = \exp \left(\frac{\mu_{\text{S}}^0|_{\text{solv}} - \mu_{\text{S}}^0|_{\text{no solv}}}{RT} - \frac{\mu_{\text{HS}}^0|_{\text{solv}} - \mu_{\text{HS}}^0|_{\text{no solv}}}{RT} \right) \quad (7)$$

where μ^0 represents the standard-state chemical potential and the subscripts S, HS, solv, and no solv stand for empty sites or adsorbed hydrogen in the presence or absence of solvent, respectively. Eqs. (6) and (7) can, in principle, account for non-idealities due to numerous factors, including solvent polarity and dielectric constant, if such factors can be related to the standard-state chemical potentials. In the absence of any solvent effects, α has a value of unity and the surface coverage is dependent only on the partial pressure of hydrogen and is independent of hydrogen solubility. However, α is not unity when certain solvent effects are present and under these conditions it is equal to $H_{\text{H}_2}^{-1/2}$, where H_{H_2} is the Henry's law constant for H_2 . Substitution of Eq. (7) into Eq. (6) and utilization of Henry's law indicate that the surface coverage of hydrogen is determined by the concentration of hydrogen in the liquid phase, thus increasing the liquid-phase hydrogen solubility at a constant partial pressure of hydrogen would increase the surface coverage of hydrogen [60]. The study of Cerveny

et al. represents one of the few that has examined this topic experimentally as it involved H_2 chemisorption at 300 K on a catalyst suspended in various solvents, and the results are presented in Fig. 5, which shows that the surface concentration of adsorbed hydrogen is proportional to the concentration of H_2 in the bulk liquid phase over a 13-fold variation in H_2 solubility [61]. However, the concentration of surface Pt atoms is only 0.26 mmol/g cat if 100% dispersion is assumed; therefore, in this 5% Pt/activated carbon catalyst either the ordinate is incorrect or most of the adsorbed hydrogen resides on the carbon, rather than the Pt surface assuming no impurities were present. This discrepancy, which was not addressed by the authors, cannot be attributed to a procedural error because their H_2 solubility measurements, in the absence of a catalyst, were in excellent agreement (within 5%) with H_2 solubility data reported in the literature. In spite of this discrepancy, the results show that the liquid-phase H_2 concentration can affect the surface concentration of adsorbed hydrogen at a constant partial pressure of hydrogen. Recently Bradley and Busser reported another technique to determine H_2 chemisorption and the H_2 - O_2 titration reaction on heterogeneous catalysts in the liquid phase, and this represents another approach that could be used to determine the effect of H_2 solubility on the surface coverage of hydrogen [62].

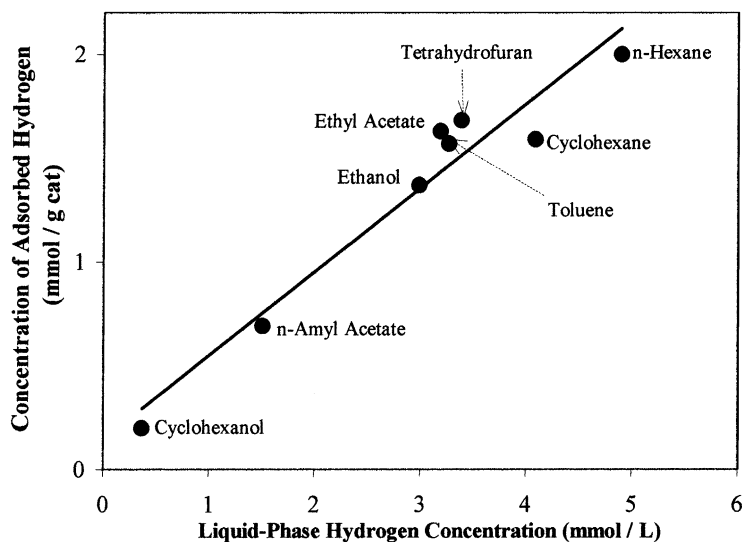


Fig. 5. Effect of liquid-phase H_2 concentration on the concentration of hydrogen adsorbed on 5% Pt/carbon at 300 K and 1 atm H_2 (from [60]).

In the context of the previous discussion, it is difficult to reconcile the absence of solvent effects on Pd based only on equilibrium arguments. It is apparent from Eq. (7) that α is unity if the solvent effect on the adsorbed state and the vacant sites is identical and thereby cancel out, i.e. the difference between the standard-state chemical potential of the vacant site in the presence of solvent and that in the absence of solvent is identical to the difference between the standard-state chemical potential of adsorbed hydrogen in the presence and that in the absence of solvent. Consequently, we speculate that the absence of solvent effects with Pd indicates that solvent effects affect the vacant site and the adsorbed hydrogen similarly, hence essentially canceling out the non-ideality and yielding a value of unity for α . Alternatively, one might argue that solvent effects on the vacant site and the adsorbed hydrogen are negligible during cyclohexene hydrogenation over Pd; therefore, α is unity and the surface coverage of hydrogen is independent of the liquid-phase H_2 concentration. More studies are clearly needed to better understand metal specificity on solvent effects. Presently, it is difficult to predict solvent effects a priori, and additional kinetic studies free of transport limitations are needed to quantify these effects. Finally, solvent effects can also play an important role during reaction in a supercritical medium and reviews on this subject have been published recently [63,64].

4. Kinetics of C=C and C=O bond hydrogenation

As mentioned, this review will focus on the kinetics of liquid-phase hydrogenation of unsaturated organics, with a particular emphasis on α,β -unsaturated aldehydes. The issues related to chemoselective hydrogenation of the C=O bond for these systems have been studied extensively; however, detailed kinetics have been obtained only recently [1,7,8,12]. The kinetics of liquid-phase hydrogenation of olefinic and aromatic hydrocarbons have been studied in some detail [24–26,44,49,54–56,61,65–70], but they will not be stressed in the present work.

The microkinetic study of ethylene hydrogenation over supported Pt catalysts serves as a satisfactory starting point for a discussion of the kinetics of liquid-phase hydrogenation reactions because a number of

assumptions made in rationalizing liquid-phase kinetics are based on these studies [71,72]. The kinetics for ethylene hydrogenation exhibits near zero-order dependence on ethylene pressure at low temperatures (below 273 K) and high ethylene partial pressure, while negative reaction orders are observed at higher reaction temperatures (above 300 K). Furthermore, the order with respect to hydrogen pressure increases from 0.5 at low reaction temperatures to 1.1 at higher temperatures. The kinetics were modeled using a sequence of elementary reaction steps consistent with surface science, kinetic and isotopic exchange studies. These microkinetic studies assumed dissociative adsorption of hydrogen, stepwise addition of H atoms, and competitive as well as non-competitive adsorption between ethylene and hydrogen. Reaction at temperatures below 300 K resulted in saturation coverage of ethylene on the sites for competitive adsorption leaving only the non-competitive sites available for hydrogen adsorption. Reaction at higher temperatures resulted in significant desorption of ethylene making the competitive adsorption sites also available for H adsorption. Furthermore, the reversibility of H adsorption on non-competitive sites decreased with increasing temperature. The microkinetic studies of Dumesic and co-workers rationalized wide variations in reaction orders with respect to ethylene and hydrogen, and their results highlight the important mechanistic information that can be gained from such kinetic studies [71,72]. Although the liquid-phase hydrogenation reaction kinetics of more complex organic compounds can be more complicated, some of the concepts gained from microkinetic studies are useful.

A recent investigation of liquid-phase citral hydrogenation over supported Pt catalysts also emphasizes the importance of studying reaction kinetics [7,8,12]. Fig. 6 displays the significant reaction pathways for citral hydrogenation, which constitute a complex network of parallel and series reactions. Thermodynamic arguments indicate that the isolated C=C bond should be the easiest to hydrogenate followed by the conjugated C=C bond and finally the C=O bond. Detailed kinetic studies, in the absence of transport limitations and poisoning effects, were performed using SiO_2 - and TiO_2 -supported Pt catalysts, and they showed that reaction temperature can have an unusual effect on the reaction rate and can also significantly alter product distribution. In contrast to conventional Arrhenius

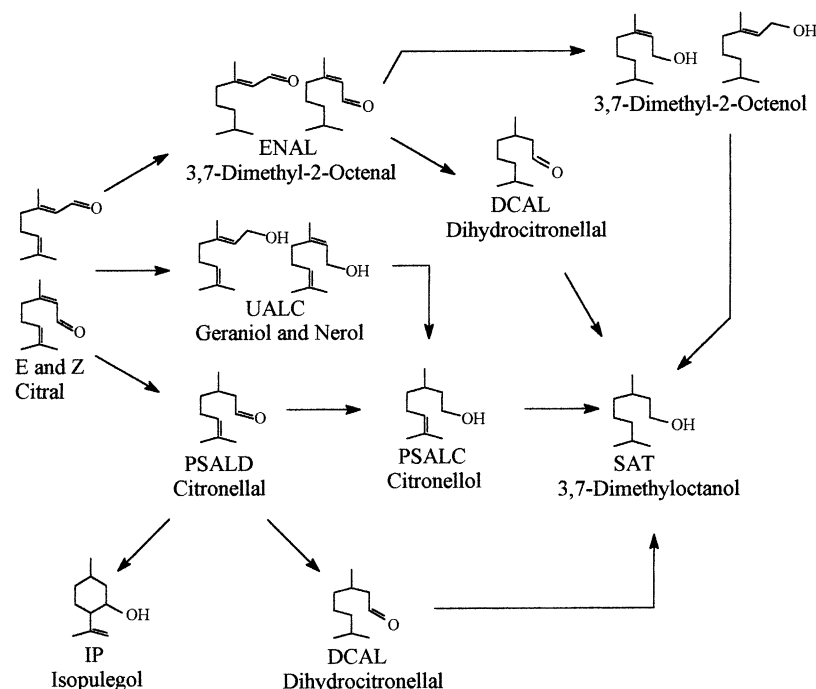


Fig. 6. Reaction network for citral hydrogenation.

behavior, citral hydrogenation exhibits an activity minimum as temperature increases from 298 to 423 K, as shown in Fig. 7a, which displays the TOF for H_2 uptake during reaction over 1.44% Pt/SiO₂ at 20 atm H_2 . The initial TOF for H_2 uptake during this reaction 298 K was 0.6 s^{-1} , but the rate decreased by an order of magnitude during the first 4 h of reaction after which time 50% conversion was achieved. In contrast, citral hydrogenation at 373 K exhibited a very high TOF during the first minute of reaction after which time it reached 0.02 s^{-1} and remained constant with negligible deactivation up to 80% conversion. The initial TOF at 423 K was higher than that observed at 373 K and gave an activation energy of 7 kcal/mol with no significant deactivation being detected. The rates displayed in Fig. 7a are based on the total H_2 uptake and include contributions from hydrogenation of citral as well as the intermediates, including geraniol, nerol, and citronellal. The rate based on citral disappearance also exhibits an activity minimum, as shown in Fig. 7b, which plots the initial rate of citral disappearance at conditions identical to those in Fig. 7a. This unusual behavior could not be attributed to

artifacts arising from transport limitations or poisoning effects because the Madon–Boudart test verified their absence under reaction conditions. Similar unusual behavior was also observed during hydrogenation of citronellal, geraniol and nerol, as shown in Table 3. The rates for citral and geraniol hydrogenation were significantly higher at 298 K compared to 373 K. For both of these reactions, an extremely high rate occurred during the first minute of reaction at 373 K after which time pseudo-steady-state behavior was realized and respective TOFs of 0.15 and 0.005 s^{-1} were measured for citral and geraniol disappearance.

Table 3
Initial rate for citral, citronellal, and geraniol hydrogenation over Pt/SiO₂ at 298 and 373 K with 20 atm H_2 and 1 M citral in hexane [8]

	TOF at 298 K (s^{-1})	TOF at 373 K (s^{-1})
Citral	0.19	0.015
Geraniol	1.2	0.005^a
Citronellal	0.11	0.07

^a Evaluated after the high activity period during the first minute of reaction.

The hydrogenation rates of the organic compounds listed in Table 3 along with values obtained during competitive hydrogenation of a mixture of these organics suggested that decomposition of the unsaturated alcohol isomers to form CO is responsible for the activity minimum because adsorbed CO inhibits the reaction [8].

Decreases in activity with increasing temperature have been reported previously for other hydrogenation reactions; for example, the vapor-phase hydrogenation of benzene, and this behavior was attributed to a decrease in the surface coverage of adsorbed benzene at higher temperatures [73,74]. It is difficult to use a similar argument for citral hydrogenation since the

kinetics exhibit an activity minimum. A kinetic rationale to explain this unusual behavior was proposed according to the following sequence of reactions:

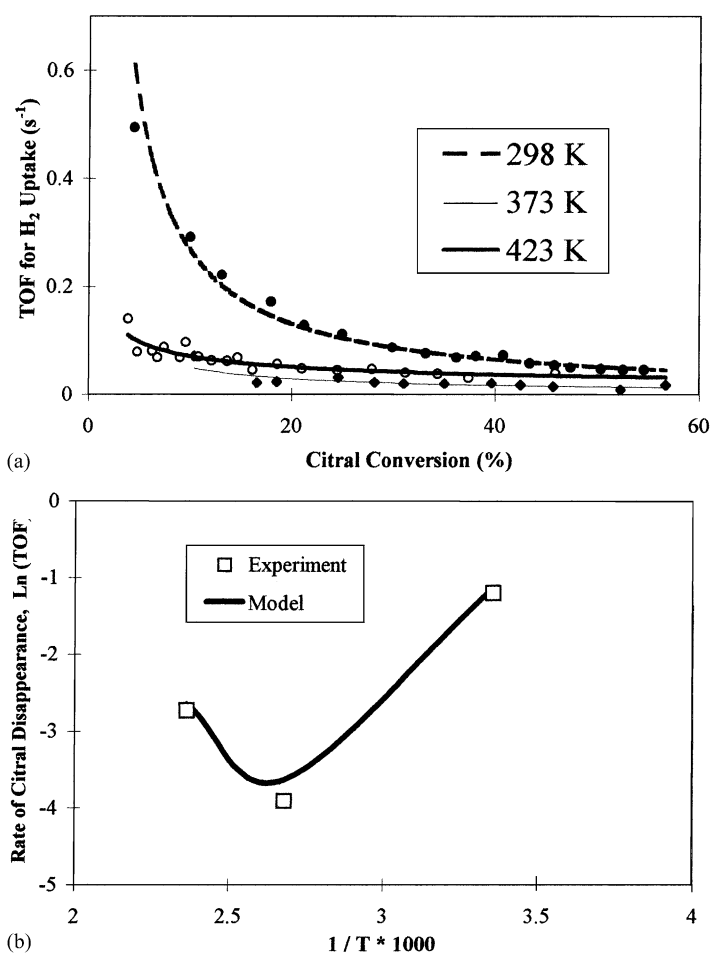
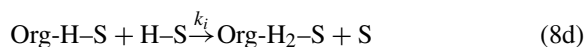
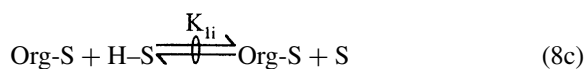
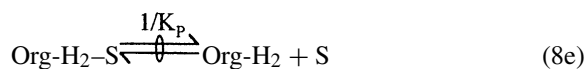


Fig. 7. Effect of temperature on (a) H₂ uptake, and (b) initial TOF for citral disappearance during citral hydrogenation over Pt/SiO₂ at 298, 373, 423 K with 20 atm H₂ and 1 M citral in hexane (from [7]).



which was used to model each of the individual hydrogenation reactions in Fig. 6. The symbols Org, Org-S, H-S, K_i , K_{1i} , and k_i represent the organic that is hydrogenated in step i , the adsorbed organic, adsorbed hydrogen, the adsorption equilibrium constant for species i , an equilibrium constant for formation of the half-hydrogenated species, and the intrinsic rate constant for addition of the second H atom, respectively. Assuming quasi-equilibrium for adsorption of hydrogen and formation of the half-hydrogenated species, addition of the second H atom as the rate determining step, and competitive adsorption between hydrogen and the organic, the following rate expression was obtained:

$$r_i = k_i K_{1i} K_{\text{Org}} K_{\text{H}} C_{\text{Org}} P_{\text{H}_2} \theta_s^2 \quad (9)$$

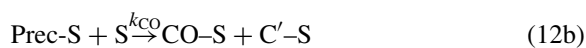
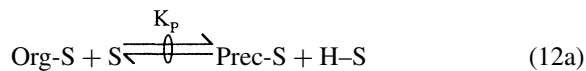
where θ_s is the fraction of vacant surface sites. The site balance was obtained by assuming that the principal surface species were citral and CO and the surface coverage of all other species was negligible, thus yielding the following expression for θ_s :

$$\theta_s = \frac{1 - \theta_{\text{CO}}}{1 + K_{\text{Citral}} C_{\text{Citral}}} \quad (10)$$

where θ_{CO} is the surface coverage of adsorbed CO. The hydrogenation rate of step i in Fig. 6 is then described as follows:

$$r_i = \frac{k_i^{\text{app}} C_{\text{Org}}}{(1 + K_{\text{Citral}} C_{\text{Citral}})^2} (1 - \theta_{\text{CO}})^2 \quad (11)$$

The hydrogen pressure terms were incorporated into the apparent rate constant because the kinetics shown in Fig. 7 were obtained at a constant H_2 pressure. The surface coverage of CO was described by a sequence of steps consistent with the surface science studies of Barteau and co-workers [75,76].



where Org-S, Prec-S, and C'-S are the adsorbed organic that is undergoing decarbonylation, the precursor prior to decarbonylation, and the carbonaceous species resulting from the decarbonylation reaction, respectively. The unsaturated alcohol isomers (geraniol and nerol) are the most likely to be undergoing decomposition; however, citral decomposition cannot be completely discounted. Assuming quasi-equilibrium for the precursor formation, the rate of CO formation can be written as follows:

$$\frac{d\theta_{\text{CO}}}{dt} = \frac{k_{\text{CO}} K_{\text{P}} K_{\text{Org}} C_{\text{Org}} \theta_s^2}{K_{\text{H}_2}^{1/2} P_{\text{H}_2}^{1/2}} - k_{\text{D}} \theta_{\text{CO}} \quad (13a)$$

$$\frac{d\theta_{\text{CO}}}{dt} = k'_{\text{CO}} C_{\text{UALC}} \theta_s^2 - k_{\text{D}} \theta_{\text{CO}} \quad (13b)$$

where C_i , θ_{CO} , θ_s , k'_{CO} , and k_{D} are the concentration of species i , the fractional surface coverage of CO, the fraction of vacant sites, the apparent rate constant for decarbonylation of the precursor, and the intrinsic rate constant for CO desorption. The equations listed above were fit to the temporal concentration profile obtained during citral hydrogenation at 20 atm H_2 and 298, 373, and 423 K, and the fit is shown in Fig. 8. The optimization routine yielded thermodynamically consistent parameters based on criteria that will be discussed later. The assumptions used in formulating the rate expression are consistent with the microkinetic studies for ethylene hydrogenation discussed earlier.

Dissociatively adsorbed hydrogen on Group VIII metals is well established, and this form of hydrogen is frequently invoked for modeling hydrogenation reactions [77]. There have been reports that have utilized non-dissociatively adsorbed hydrogen, including Eley-Rideal kinetics [78]; however, the validity of the latter kinetic model remains to be verified. Competitive adsorption between hydrogen and the organic was assumed, consistent with the study of ethylene hydrogenation on Pt that indicates, as discussed previously, a strong contribution of the competitive adsorption mechanism at reaction temperatures above 300 K [72,73]. Furthermore, a competitive adsorption model was also capable of correlating reaction kinetics for citral hydrogenation over TiO_2 -supported Pt catalysts which displayed a negative first-order dependency with respect to citral concentration. This behavior could be explained only by a competitive adsorption model because the non-competitive adsorption model

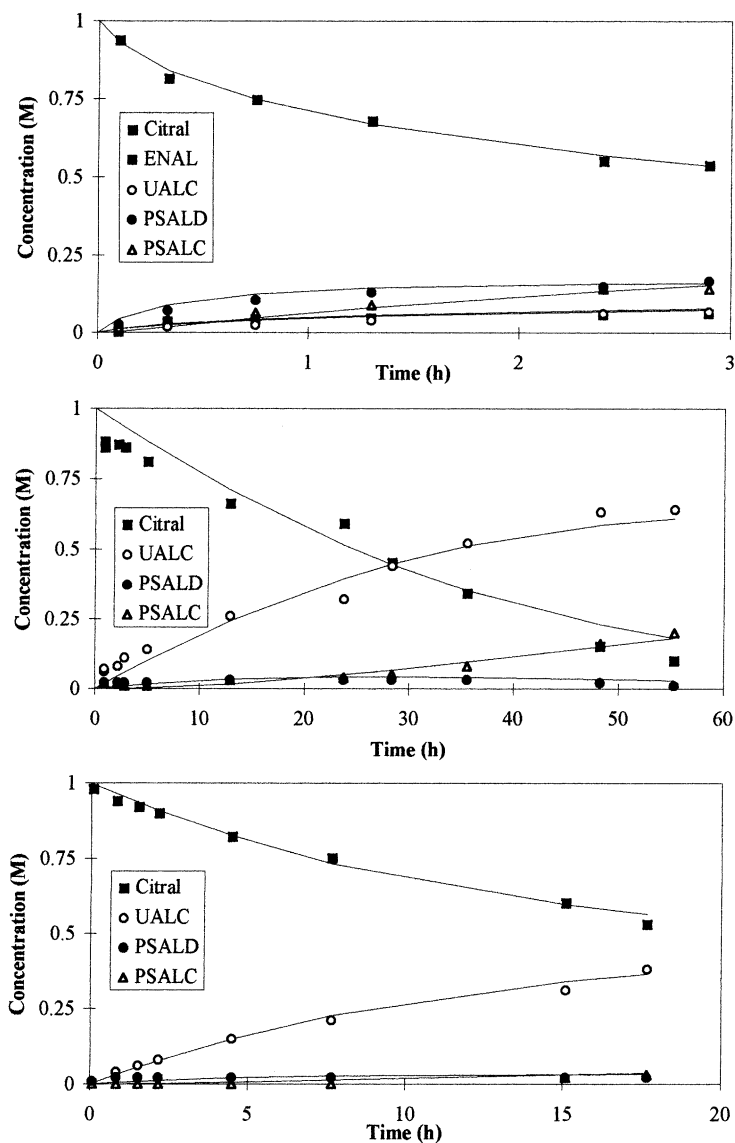


Fig. 8. Fit of kinetic model (Eqs. (11) and (13)) to experimental data for reaction over Pt/SiO₂ at 20 atm H₂, 1 M citral in hexane, and (a) 298 K, (b) 373 K, and (c) 423 K. Symbols represent experimental data while solid lines represent the model prediction.

was incapable of yielding negative reaction orders [12]. The assumption of the addition of the second H atom as the RDS is also reasonable because the microkinetic study of ethylene hydrogenation indicated that the addition of the second H atom was slower than the addition of the first [72]. Although the difference in the rates of addition of the first and second H atoms is not large in the microkinetic study, the

results of Sato and Miyahara for ethylene hydrogenation over Ni indicate that the rate of addition of the first H atom to ethylene is more than an order of magnitude higher than the rate of the addition of the second H atom [72,79]. Furthermore, the initial rate for citral hydrogenation exhibits a first-order dependency on hydrogen pressure that can only be explained by the addition of the second H atom or dissociative H₂

adsorption as the rate determining step. It is unlikely that the latter is the RDS because this would predict a negative first-order dependency on citral concentration, in contrast to the observed zero-order dependency. To make such a RDS consistent with the observed kinetics, one must postulate that the surface coverage of all organics is negligible, which is highly unlikely. Such comparisons of vapor- and liquid-phase reaction kinetics under dramatically different reaction conditions should be conducted with caution; however, the fact that the assumptions used in the formulation of this model are consistent with those in the microkinetic study of simple olefin hydrogenation lends further support to the model proposed for organic compounds.

The activity minimum shown in Fig. 7 can be physically explained by CO inhibition using the sequence of reactions steps shown in Eqs. (12a)–(12d). The apparent activation energy of the decarbonylation reaction (Eq. (12c)) was 7 kcal/mol while that for CO desorption (Eq. (12d)) was chosen as 26 kcal/mol based on surface science results [80,81]. This low activation barrier for CO decarbonylation together with the high activation energy for CO desorption suggests that CO can be formed slowly at 300 K and remain adsorbed on the catalyst surface. At 373 K, the rate of CO formation is much higher, which results in a larger fraction of active sites being inhibited by adsorbed CO but the rate of CO desorption is also enhanced at 373 K; hence, a portion of CO formed under reaction conditions can desorb from the catalyst surface to yield a pseudo-steady-state situation between the rates of CO formation and CO desorption. At higher reaction temperatures, above 373 K, the rate of CO desorption is further enhanced relative to that for CO formation thus freeing a larger fraction of active sites for the hydrogenation reaction and yielding conventional Arrhenius behavior.

Kinetic studies with supported metal catalysts [7,82,83], and spectroscopic studies with single crystal surfaces [75,76,84,85] have shown evidence for CO inhibition under reaction conditions. Fig. 9 displays the temporal concentration profile during citral hydrogenation over Pt/SiO₂ at 300 K and 1 atm H₂. A 20-fold decrease in rate occurs during the first 4 h of reaction due to adsorbed CO generated from the decomposition of either citral or the unsaturated alcohol. Purging the reactor with air oxidized the adsorbed CO

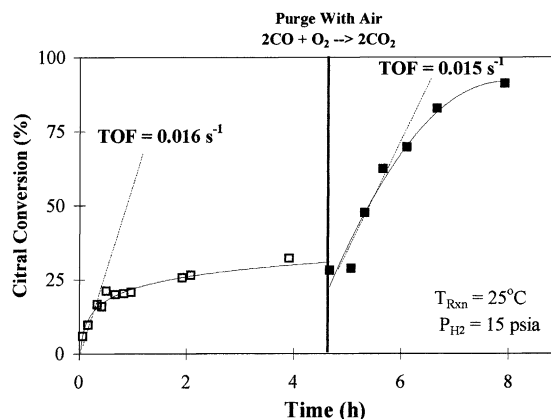


Fig. 9. Temporal citral conversion profile for citral hydrogenation over 3.80% Pt/SiO₂ at 300 K with 1 atm H₂ and 0.06 M citral in hexane. An amount of 1000 sccm of air was purged through the reactor after 5 h of reaction, which restored the initial activity.

to CO₂, and the initial activity was recovered. Lercher and co-workers had performed an identical experiment during crotonaldehyde hydrogenation over Pt at higher pressures and they obtained similar results [82]. Further studies indicated that a catalyst inhibited by CO prior to the start of the reaction exhibited a TOF which was an order of magnitude lower than that obtained with a catalyst that had not been exposed to CO [18]. Eqs. (12a) and (12b) indicate the presence of a precursor prior to decarbonylation. Spectroscopic studies with single crystals have indicated the presence of acyl [75,76], oxametallocycle [84], and η³-alkoxide [85] surface species during alcohol and aldehyde decomposition reactions. Spectroscopic characterization of the solid–liquid interface with supported metal catalysts under liquid-phase reaction conditions is very difficult and it has not been possible to study the structural aspects of the precursor species; nevertheless, the kinetic rationale just presented is capable of producing the observed activity minimum because the activation barrier for the decarbonylation reaction is lower than that for CO desorption.

A good fit of the model to experimental data is a necessary, but not a sufficient, criterion to validate a model. When possible, enthalpies and entropies of adsorption based on the adsorption equilibrium constants should also be evaluated and the thermodynamic consistency of these values should be examined (using a standard state of 1 atm). These standard-state

transformations have been addressed before and have been performed with the parameters obtained from the non-linear regression of citral hydrogenation reaction kinetics as well as with those for liquid-phase benzene hydrogenation [7,60,86]. Thermodynamic arguments show that the parameters extracted from the non-linear regression must satisfy three criteria [87,88]. First, the enthalpy and entropy of adsorption should be negative. Second, the entropy of adsorption, after correcting for the standard-state, must be less than the standard entropy of the species in the gas phase. Third, the minimum entropy loss upon adsorption should be about 10 e.u. due to a loss of at least one degree of translational freedom upon adsorption [87,88]. All three of these criteria were satisfied for the parameters obtained during citral hydrogenation [7]. A comparison of enthalpies and entropies of adsorption obtained from liquid-phase reaction kinetics to those from vapor-phase kinetics for benzene hydrogenation over supported Pd catalysts is presented in Table 4. No significant differences are apparent between the vapor-phase and liquid-phase parameters when the same standard state is used. In both cases, the heat of adsorption of benzene and weakly adsorbed hydrogen are consistent with the values obtained from calorimetric measurements.

In conjunction with the unusual effect on rate, temperature also had a significant effect on the product distribution, as shown in Table 5 which displays the selectivity to various products at a citronellal conversion of 20% over Pt/SiO₂ at 20 atm H₂ and either 298 or 373 K. The values listed in Table 5 represent a snapshot of the reaction at 20% conversion; however, the only significant change at higher conversions was the subsequent hydrogenation of citronellol and dihydrocitronellal into the completely saturated product

Table 4

Comparison of enthalpy and entropy of adsorption, at standard state of 1 atm in the gas phase, obtained from the fitted parameters for liquid- and vapor-phase benzene hydrogenation over Pd/η-Al₂O₃ catalyst [59,71]

Adsorption equilibrium constants	Vapor phase ^a		Liquid phase	
	ΔH_{ads}^0	ΔS_{ads}^0	ΔH_{ads}^0	ΔS_{ads}^0
K_{Benzene}	-20	-34	-19	-49
K_{Hydrogen}	-2	-15	-7	-25

^a [71].

Table 5

Product distribution during liquid-phase citronellal hydrogenation over Pt/SiO₂ at 298 or 373 K, 20 atm H₂, 1 M citral in hexane, and 20% conversion [8]

Product	298 K	373 K
Citronellol	21	60
Dihydrocitronellal	59	0
3,7-Dimethyloctanol	20	0
Isopulegol	0	40

(3,7-dimethyloctanol). It is apparent that higher reaction temperatures enhance selectivity for C=O bond hydrogenation while lower reaction temperatures favor C=C bond hydrogenation. At 298 K, respective selectivities of 21 and 59% were obtained for citronellol (C=O bond hydrogenation) and dihydrocitronellal (C=C bond hydrogenation). In contrast, no products arising from C=C bond hydrogenation were detected at 373 K. This behavior can be qualitatively understood from the differences in bond dissociation energies and heats of adsorption for coordination via the C=C and C=O bonds. The dissociation energy of the C=O bond is 33 kcal/mol larger than that for the C=C bond, so it is reasonable to expect that higher reaction temperatures would give a greater enhancement for C=O bond hydrogenation. Furthermore, the heat of adsorption for coordination via the C=C bond, for example, 9 kcal/mol for ethylene [89], is lower than that via C=O bond, for example, 16 kcal/mol for formaldehyde [90]. Qualitatively, this means that higher temperatures may favor adsorption via the C=O bond compared to the C=C bond. Similar behavior is also observed during citral hydrogenation over Pt/SiO₂ at 298 and 373 K and 20 atm H₂ [7]. The product distribution at 298 K reveals that the principal product is citronellal (hydrogenation of the conjugated C=C bond), whereas that at 373 K it is geraniol (hydrogenation of the C=O bond). The reason for the increase in selectivity with increasing conversion is not entirely clear; however, it has been suggested that rapid modification of the catalyst surface can take place during the initial stages of the reaction resulting in deposition of carbonaceous species which can either sterically or electronically hinder adsorption via the conjugated C=C bond, hence favoring adsorption and hydrogenation of the C=O bond [91]. No significant pressure effect on selectivity was detected during

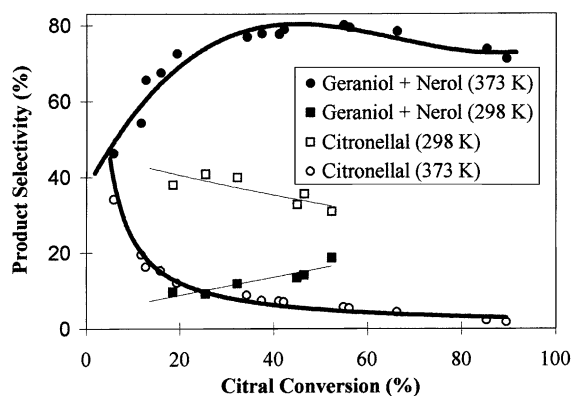


Fig. 10. Selectivity to unsaturated alcohol isomers (geraniol and nerol), and citronellal during reaction over Pt/SiO₂ at 298 and 373 K, 20 atm H₂ and 1 M citral in hexane.

citral hydrogenation over Pt/SiO₂ because the product distribution at 298 K and 1 atm H₂ was similar to that at 20 atm H₂ when compared at 20% conversion. This implies that the reaction orders in H₂ for the formation of citronellal and the unsaturated alcohol isomers (geraniol and nerol) are similar [18] (Fig. 10).

Metal–support interactions (MSI) can also significantly alter reaction kinetics, and they have been utilized to increase selective hydrogenation of the C=O bond [92,93]. During the past two decades, a significant effort has been devoted to the study of MSI (aka SMSI), which can be induced in titania-supported Group VIII metals by reduction at high temperatures, i.e. 773 K. Under these conditions oxygen vacancies form and coordinatively unsaturated cations are created, particularly at the metal–support interface, and migration of the partially reduced support, TiO_x, onto the metal can occur which causes suppression of H₂ and CO chemisorption due to site blockage [92]. MSI markedly enhanced the TOF for citral hydrogenation. Pt/SiO₂, Pt/TiO₂-LTR (low-temperature reduction at 473 K), and Pt/TiO₂-HTR (high-temperature reduction at 773 K) exhibited TOFs of 0.004, 0.02, and 1.0 s⁻¹, respectively, at 373 K, 20 atm H₂ and 1 M citral. Similar enhancements in TOF have also been observed during the vapor-phase hydrogenation of acetone, crotonaldehyde and aromatics with a carbonyl bond [93–95]. These rate enhancements were attributed to the creation of new active sites at the metal–support interface, in the form of coordinatively unsaturated cations (Ti²⁺, Ti³⁺), that could inter-

act with the lone pair of electrons on the carbonyl oxygen, polarize the C=O bond, and hence facilitate its hydrogenation. Liquid-phase citral hydrogenation over Pt/TiO₂-LTR exhibited an activity minimum with respect to temperature similar to that observed over Pt/SiO₂; in contrast, Pt/TiO₂-HTR gave conventional Arrhenius behavior with an activation energy of 18 kcal/mol. Furthermore, Pt/SiO₂ and Pt/TiO₂-LTR exhibited zero-order and first-order dependencies on citral concentration and hydrogen pressure, respectively, whereas Pt/TiO₂-HTR gave negative first-order and near zero-order dependencies on citral concentration and hydrogen pressure, respectively. A kinetic model similar to that used previously to describe the kinetics over Pt/SiO₂ was utilized. Quasi-equilibrium for dissociative hydrogen adsorption, competitive adsorption between hydrogen and citral, and the addition of the first H atom as the RDS were assumed. The surface coverage of H atoms could no longer be neglected because the near zero-order dependence with Pt/TiO₂-HTR indicates a high surface site coverage of hydrogen. The resulting rate expression was

$$r = \frac{kK_{\text{Cit}}K_{\text{H}}^{1/2}C_{\text{Cit}}P_{\text{H}}^{1/2}}{(1+K_{\text{Cit}}C_{\text{Cit}}+K_{\text{H}}^{1/2}P_{\text{H}}^{1/2})^2}(1-\theta_{\text{CO}})^2 \quad (14)$$

in which the expression for the surface coverage of CO was obtained from Eq. (13). Inclusion of the deactivation steps (Eqs. (12a)–(12d)) was not necessary to correlate the initial rates over Pt/TiO₂-HTR in a differential regime (less than 20% citral conversion); however, a good fit at higher conversions required that CO inhibition be taken into account. The above rate expression fit the kinetics over Pt/TiO₂-HTR catalysts well, and the resulting fitting constants also yielded thermodynamically consistent parameters [12]. The selectivity to unsaturated alcohol during citral hydrogenation over Pt/SiO₂, Pt/TiO₂-LTR and Pt/TiO₂-HTR is shown in Fig. 11. Pt/SiO₂ exhibits a markedly lower initial selectivity to the unsaturated alcohol isomers (geraniol and nerol) compared to Pt/TiO₂-LTR and Pt/TiO₂-HTR, and the 40% initial selectivity to the unsaturated alcohol isomers is accompanied by approximately 40% selectivity to citronellal. The absence of citronellal over TiO₂-supported Pt may be due either to deactivation of those sites on TiO₂-supported catalysts that are responsible for C=C bond hydrogenation or to a difference in crystallite morphology between

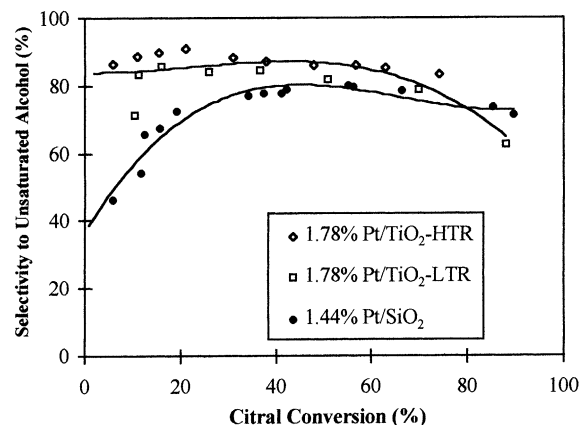


Fig. 11. Selectivity to unsaturated alcohol isomers (geraniol and nerol) over Pt/SiO₂, Pt/TiO₂-LTR, and Pt/TiO₂-HTR at 373 K, 20 atm H₂ and 1 M citral in hexane.

SiO₂- and TiO₂-supported catalysts. The latter catalysts exhibited similar selectivity to the unsaturated alcohol at 373 K in spite of the significant differences in reaction rate between the LTR and HTR catalysts. The Pt/TiO₂-LTR catalyst showed a temperature effect on product distribution similar to that with Pt/SiO₂, and product distributions during citral hydrogenation on Pt/TiO₂-LTR at 298 K, 373 K and 20 atm H₂ are shown in Fig. 12. As with Pt/SiO₂, Pt/TiO₂-LTR exhibits a higher selectivity to the unsaturated alcohol isomers as temperature increases for reasons that were discussed previously. Therefore, it is not surprising that no significant difference in product distribution

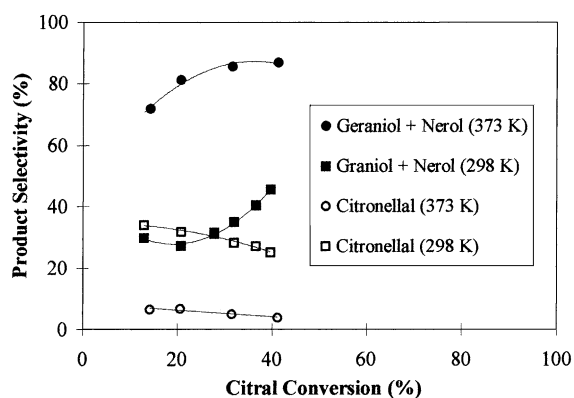


Fig. 12. Selectivity to unsaturated alcohol isomers (geraniol and nerol), and citronellal during reaction over Pt/TiO₂-LTR at 298 and 373 K, 20 atm H₂ and 1 M citral in hexane.

exists between Pt/TiO₂-LTR and Pt/TiO₂-HTR at 373 K because reaction at higher temperatures inherently favors hydrogenation of the C=O bond in citral; hence, the MSI effect on the product distribution is overshadowed by the influence of temperature.

Finally, as one would expect, the metal itself can also have a significant impact on reaction kinetics. Fig. 13 plots the initial TOF for citral hydrogenation at 1 atm versus percentage of d-character [18]. There is a 1000-fold variation in the initial TOF for citral hydrogenation among the SiO₂-supported Group VIII metals. The parameter, percentage of d-character, refers to the contribution of the d-electrons to the spd hybrid orbitals assumed in Pauling's resonance valence band theory [96], and correlations of activity versus percentage of d-character have been made previously. However, the reason for the volcano-shaped nature of the plot in Fig. 13 is not clear at this time. There are also pronounced differences in product distribution among the various metals during citral hydrogenation, and these differences have been qualitatively correlated with metal d-band widths based on the extended Huckel calculations of Delbecq and Sautet [97]. According to their arguments, the strength and geometry of adsorption are determined by the relative contributions from stabilizing two-electron interactions that involve conventional donation and back-donation processes and from destabilizing four-electron interactions that include a repulsive interaction between

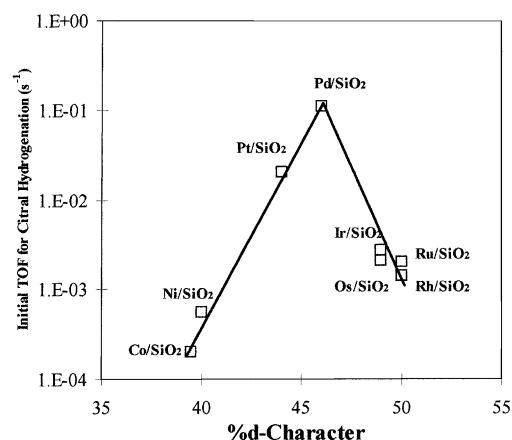


Fig. 13. Correlation of the initial TOF for citral hydrogenation with percentage of d-character. TOF was evaluated under differential conditions for citral hydrogenation at 300 K, 1 atm H₂ and 0.06 M citral in hexane.

the filled molecular orbitals of the organic molecule and the filled d-band of the metal. An increasing metal d-band width hinders adsorption via the conjugated C=C bond due to enhanced four-electron interactions and hence favors coordination via the C=O bond [97]. Among the Group VIII metals, the d-band width decreases going from left to right, i.e. Fe to Ni, and increases moving down a periodic table, i.e. Fe to Os [98]. In agreement with these trends, Ni, Pd, and Rh possess the highest initial selectivity for hydrogenation of only the conjugated C=C bond while Os exhibits the highest selectivity for C=O bond hydrogenation.

In summary, liquid-phase hydrogenation kinetics can be complex and are further complicated by solvent effects and metal–support interactions that can significantly affect product distributions and reactions rates. Quantitative kinetic analysis, in the absence of transport limitation, and mechanistic development of rate expressions are currently not common; hence, more work on liquid-phase hydrogenation reactions has to be focused on obtaining a better quantitative understanding of the selectivity issues.

5. Crystallite size effects

The term structure sensitivity was coined by Boudart to explain large variations in TOFs due to changes in catalyst structure brought about by varying the exposed crystal plane or by changing the average metal crystallite size over the range of 1–10 nm [99,100]. The structure sensitivity of a number of different reactions has been probed and reviewed [101–104]. In general C–C, C–O, and C–N bond scission reactions are structure sensitive while C–H bond formation and scission are structure insensitive [100,105]. Structure sensitivity has been rationalized on the basis of geometric and electronic factors; however, it has been correctly pointed out that the distinction between the two factors can become blurred since both can vary simultaneously [101]. The reasons for structure sensitivity have received considerable attention and thus will not be repeated in detail here; however, it is instructive to examine the causes for structure insensitivity [101–104,106].

It is difficult to rationalize the structure insensitivity of a number of reactions, such as hydrogenation reactions, because energetic inhomogeneity due to

surface metal atoms with varying coordination is present with supported metal catalysts. A reaction is considered structure insensitive if similar rates are detected over various crystal planes and with catalysts containing widely differing metal crystallite size, particularly in the region of 1–10 nm. In addition, Boudart has suggested that all active sites have similar catalytic activity in a structure insensitive reaction [107]. Somorjai and Carrazza have proposed two hypotheses for structure insensitivity. First, they noted that the heat of adsorption of CO on Pd(111) decreases significantly from 35 to 10 kcal/mol with increasing surface coverage due to enhancement of repulsive adsorbate–adsorbate interactions that weaken the adsorbate–surface interactions. Furthermore, since weakly adsorbed CO is present at high pressures and is involved in reactions such as CO oxidation, changes in surface structure would not be expected to have a significant impact on this reaction [108]. This idea is consistent with the structure insensitivity of benzene hydrogenation because it has been suggested that the reactive forms of both hydrogen and benzene involved in the hydrogenation reaction are those that are weakly adsorbed [109]. A second reason for structure insensitivity was the hypothesis that a structure insensitive reaction, for example, ethylene hydrogenation, does not occur on a clean metal surface, but rather on top of a carbonaceous overlayer covering the metal surface [106,110,111]. Zaera and Somorjai studied ethylene hydrogenation over Pt(111), and they suggested that ethylidyne species cover the catalyst surface and hydrogenation occurs on top of these species [110]; however, Beebe and Yates performed an in situ Infrared spectroscopic study on Pd/Al₂O₃ to show that ethylidyne was a spectator species and it did not influence the rate of ethylene hydrogenation [112]. Thomson and Webb had earlier proposed a similar working model for olefin hydrogenation [113] and it was used by Madon et al. to support their model for solvent effects during liquid-phase cyclohexene hydrogenation over Pt/SiO₂ [56]. Finally, surface restructuring can occur under reaction conditions; so, structure insensitivity might be due to the creation of new and more uniform active sites under reaction conditions. A significant consequence of restructuring is that the active sites may not be based on the nature or the structure of the clean metal surface [114,115].

The absence of a significant variation in specific activity with changing crystallographic planes or widely varying crystallite size clearly indicates structure insensitivity; however, a variation in rate with changing crystallite size or crystallographic plane does not necessarily imply structure sensitivity. Somorjai and Carrazza have discussed the possibility that the structure sensitivity of certain reactions, such as CO oxidation, depends on reaction conditions. A shift in the RDS under different reaction conditions can induce a reaction condition-dependent structure sensitivity [109].

As mentioned, hydrogenation reactions are typically considered to be structure insensitive; however, significant variation in specific activity has been observed during ethylene hydrogenation over various single crystal Ni surfaces [116]. Ni(111) and Ni(110) planes exhibit similar TOFs; however, no significant activity could be detected over Ni(100) surface. This behavior on Ni(100) was attributed to a buildup of carbonaceous deposits that completely covered the catalyst surface and prevented dissociative adsorption of hydrogen, thus yielding a completely inactive surface. Similar species were also present on the Ni(111) and Ni(110) surfaces; however, these species rearranged on these surfaces to leave surface metal atoms available for dissociative adsorption of hydrogen [116]. Some have termed such behavior as secondary structure sensitivity, which stresses a need for caution in classifying reactions as structure sensitive [117]. Liquid-phase hydrogenation over SiO₂-supported Pt is another example of a reaction which may be classified as a secondary structure-insensitive reaction. Fig. 14a shows the influence of average Pt crystallite size on the initial TOF for citral hydrogenation at 373 K, 20 atm H₂ and 1 M citral in hexane. There is a 25-fold increase in TOF as the average crystallite size increases from 1 nm (H/Pt = 1.0) to 5 nm (H/Pt = 0.22), but further increases in TOF as the average crystallite size increased from 5 to 30 nm was minimal as only a two-fold variation occurred in this region. In contrast, this trend is not observed at 298 K, as shown in Fig. 14b which shows the TOF for H₂ uptake during the course of reaction at 20 atm H₂ and 1 M citral in hexane [118]. No significant deactivation was detected during reaction at 373 K; therefore, only initial rates are displayed in Fig. 14a. In contrast, substantial deactivation was observed at 298 K, so it is not possible

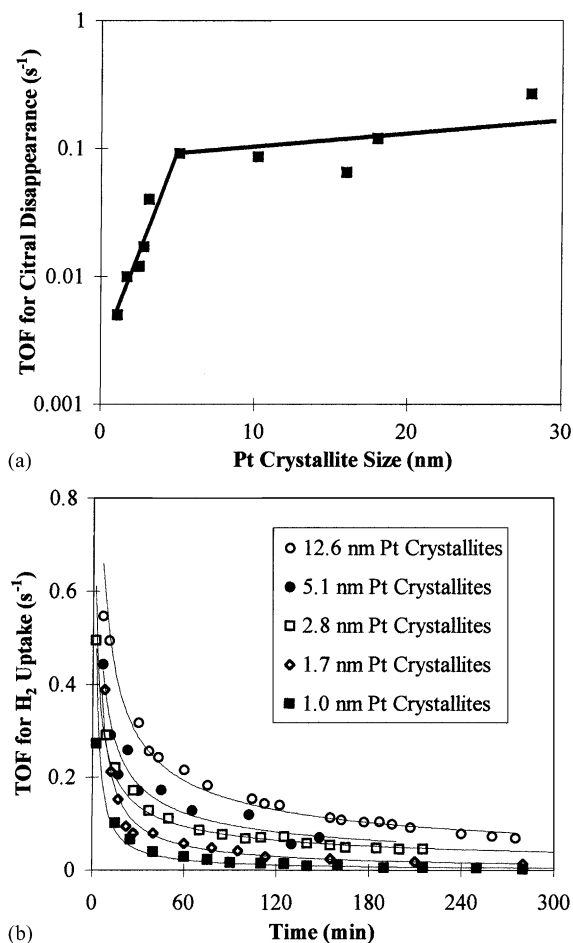


Fig. 14. Effect of average crystallite size, determined from H₂ chemisorption, on (a) TOF for citral disappearance at 373 K, and (b) TOF for H₂ uptake 298 K with 20 atm H₂ and 1 M citral in hexane.

to report a single representative TOF value for a given catalyst. This brings up two points. First, caution must be exercised when activities are measured at only one set of reaction condition to probe crystallite size effects because this yields no information about reaction kinetics and the data may be gathered in the mass transfer limited regime. Secondly, it is important to examine the progress of the reaction because deactivation behavior, such as that shown in Fig. 13b, can complicate accurate evaluation of TOFs. The crystallite size effect at 373 K can also be explained by the kinetic model proposed earlier to explain the activity minimum

during citral hydrogenation on Pt/SiO₂. In conjunction with the hydrogenation reaction, it was proposed that there is a parallel decomposition pathway that yields adsorbed CO, which can inhibit active sites for the hydrogenation reaction. Furthermore, it was asserted that there is a greater surface coverage of CO at 373 K as compared to 298 K, at least at shorter reaction times, which results in a lower activity at 373 K. Similarly, the lower TOF at 373 K with the highly dispersed catalyst may be due to a greater surface coverage of adsorbed CO and hence a lower concentration of active sites available for citral hydrogenation. A large fraction of highly dispersed surface atoms consist of those with low coordination numbers in the form of kink, edge, and step sites, and the relative amount of these sites decreases with increasing crystallite size [119]. These sites can facilitate decarbonylation reactions, as seen from the studies of 3-methyl-crotonaldehyde hydrogenation over Pt(1 1 1), (1 1 0), and (5 5 3) surfaces [120–123]. These results indicate that Pt(1 1 0), which has a furrowed structure and hence a greater number of low coordination atoms, exhibits the highest selectivity to decarbonylation products followed by Pt(5 5 3) and then Pt(1 1 1). The Pt(5 5 3) surface consists of three rows of surface atoms with a coordination number of nine, as on a Pt(1 1 1) surface, and one row of atom with coordination number of seven, as on Pt(1 1 0) surface, which give the Pt(5 5 3) surface characteristics between those of Pt(1 1 1) and Pt(1 1 0) surfaces. Therefore, it is not surprising that Pt(5 5 3) exhibits selectivities intermediate between Pt(1 1 1) and Pt(1 1 0) [120–123]. The observed selectivity over a Pt(5 5 3) surface can be accurately predicted from the product distribution over Pt(1 1 1) and (1 1 0) surfaces based on the surface statistics of the Pt(5 5 3) surface using the following equation:

$$S_{553} = \frac{3S_{111} + S_{110}}{4}$$

where S_{553} , S_{111} , and S_{110} are the selectivities for various products over Pt(5 5 3), (1 1 1), and (1 1 0) surfaces, respectively [120]. Ford et al. recently reported that while reactivity varied with the crystal face, there was no correlation between adsorption and reaction of a number of different compounds with step atom density [124]. Furthermore, they suggested that the active sites are not the step atoms alone, but rather a

collection of step and terrace atoms correctly aligned to facilitate the reaction. Regardless of the nature of the active site, it is clear that decarbonylation reactions are enhanced over corrugated surfaces and suppressed over flat surfaces. This is consistent with the results presented in Fig. 14a in which there is a marked increase in the TOF for citral hydrogenation on the 1–5 nm crystallites, i.e. the region where the fraction of Pt(1 1 1) sites in the crystallite increases rapidly thus reducing the propensity for decarbonylation reactions. Metal crystallites that are 5 nm or larger consist primarily of Pt(1 1 1) surfaces; therefore changes in TOF are minimal in this region. The absence of a crystallite size effect during citral hydrogenation over Pt/SiO₂ at 298 K is consistent with atmospheric pressure studies at 298 K over supported Pd and Ru catalysts [18,125]. This absence may be due to a slower rate of alcohol decomposition compared to the hydrogenation reaction, thus reducing the influence of the structure-sensitive decomposition reaction on the overall hydrogenation reaction kinetics.

Kinetic studies over supported metal catalysts by Lercher and co-workers [126] along with the theoretical studies of Delbecq and Sautet [97] and the surface science studies of Oudar [120] and Birchem et al. [121–123] indicate that different crystallographic planes can alter selectivity during hydrogenation of α,β -unsaturated aldehydes. These studies were conducted with crotonaldehyde and 3-methylcrotonaldehyde, and they indicate that close-packed planes such as Pt(1 1 1) are selective for C=O bond hydrogenation due to repulsive interactions between the methyl groups attached to the C=C bond and the surface. In addition, corrugated surfaces such as Pt(1 1 0) are more selective for hydrogenation of the conjugated C=C bond due to suppressed repulsive interactions [122]. An analogous effect was observed during cinnamaldehyde hydrogenation over supported Ru catalysts. The selectivity for C=O bond hydrogenation in cinnamaldehyde increased with increasing crystallite size due to repulsive interactions between the phenyl ring and the large metal crystallites which resulted in tilted adsorption of the molecule which hindered interaction via the conjugated C=C bond and enhancing interaction through the C=O bond. This effect was absent with smaller metal crystallites because the C=O and C=C bonds could approach the

surface with less repulsive interactions between the phenyl ring and the metal surface [127,128]. In view of these results, it is surprising that no crystallite size effect was observed on the product distribution during citral hydrogenation over Pt, Pd, and Ru [18,118,125] because the conjugated C=C bond is highly substituted. However, substituent effects appear to be more complicated than first thought. Based on theoretical studies [97] and vapor-phase reactions over single crystal and supported metal catalysts [121,129,130], the presence of a methyl substituent on the conjugated C=C bond can hinder adsorption via the conjugated C=C bond. Beccat et al. have shown by a comparison of crotonaldehyde and methylcrotonaldehyde that the presence of a methyl group in place of a hydrogen atom on the conjugated C=C functionality decreases the hydrogenation rate of the C=C bond four-fold and increases the rate of hydrogenation of the C=O bond four-fold. In addition, their results indicate a 10-fold decrease in the rate for hydrogenation of the C=C bond in methylcrotyl alcohol compared to crotyl alcohol [129]. However, in spite of the bulky substituent groups present at the conjugated C=C bond of citral, liquid-phase studies at 300 K at 1 atm H₂ showed that the primary product was citronellal (which arises from hydrogenation of the conjugated C=C bond) [18]. This issue becomes even more puzzling in light of de Jesus and Zaera's detailed spectroscopic study of acrolein and crotonaldehyde adsorption on a Pt(1 1 1) surface. In spite of the methyl group present at the conjugated C=C bond of crotonaldehyde, the results of de Jesus and Zaera indicate that it adsorbs via the C=C bond while acrolein, which has only H atoms attached to the conjugated C=C bond, adsorbs parallel to the surface [131].

In summary, the kinetics of some hydrogenation reactions appear to exhibit a dependence on crystallite size; however, these reactions should not necessarily be considered structure sensitive because the apparent crystallite size effect can be attributed to an accompanying side reaction that inhibits active sites for hydrogenation. Crystallite size effects also appear to influence product distribution and for α,β -unsaturated aldehyde hydrogenation such an effect has routinely been ascribed to the influence of substituent groups, in contrast to the unusual behavior recently reported by de Jesus and Zaera.

6. Summary

The kinetics of liquid-phase hydrogenation reactions were reviewed with a particular emphasis on hydrogenation of α,β -unsaturated aldehydes. The following aspects were emphasized.

1. Prior to obtaining accurate kinetics with supported metal catalysts, it is essential to ensure the absence of all transfer limitations by application of an appropriate test, such as the Madon–Boudart method which checks for external and internal heat and mass transfer resistances, and/or the Weisz criterion, or an effectiveness factor based on the Thiele modulus. Transport limitations can significantly affect reaction kinetics and alter product distributions, as shown by a case study of enantioselective ethyl pyruvate hydrogenation.
2. The mechanistic basis of solvent effects in heterogeneously catalyzed hydrogenation reactions is not well understood, but these effects can influence reaction kinetics via bulk fluid-phase interactions as well as by competitive adsorption with the reactants. Thermodynamic arguments were addressed which indicate that in the presence of quasi-equilibrium between H₂ in the gas phase, the liquid phase, and the adsorbed state, solvent effects can influence the surface coverage of hydrogen at a constant partial pressure of H₂. In the absence of solvent effects, the surface coverage of hydrogen is independent of the liquid-phase H₂ concentration and is a function of only the partial pressure of H₂ in the gas phase.
3. Liquid-phase hydrogenation reactions can be complex and influenced by a number of factors including, but not limited to, process parameters, side reactions, metal–support interactions, and metal specificity. It is important to study reaction dynamics to properly understand these effects because significant changes in activity and product distribution can occur during reaction.
4. Hydrogenation reactions are typically assumed to be structure insensitive; however, examples were discussed in which hydrogenation reactions are dependent on crystallite size and exposed crystal plane. Such behavior during liquid-phase hydrogenation of citral was attributed to an inhibiting side reaction occurring concurrently with the hydrogenation reaction.

Acknowledgements

This study was supported by the DOE, Division of Basic Energy Sciences under Grant no. DE-FE02-84ER13276.

References

- [1] R.A. Sheldon, *J. Mol. Catal. A: Chem.* 107 (1996) 75.
- [2] R.N. Landau, U.K. Singh, F. Gortsema, Y. Sun, S.C. Gomolka, T. Lam, M. Futran, D.G. Blackmond, *J. Catal.* 157 (1995) 201.
- [3] M. Ash, I. Ash, *Specialty Chemicals Handbook*, 1st Edition, Vol. 1, Synapse Information Resources, New York, 1997.
- [4] H.-U. Blaser, H.-P. Jalett, F. Spindler, *J. Mol. Catal. A: Chem.* 107 (1996) 85.
- [5] M. Besson, C. Pinel, *Top. Catal.* 5 (1998) 25.
- [6] P. Gallezot, D. Richard, *Catal. Rev. Sci. Eng.* 40 (1998) 81.
- [7] U.K. Singh, M.A. Vannice, *J. Catal.* 191 (2000) 165.
- [8] U.K. Singh, M. Sysak, M.A. Vannice, *J. Catal.* 191 (2000) 181.
- [9] R.L. Augustine, *Catal. Today* 37 (1997) 419.
- [10] C.R. Landis, J. Halpern, *J. Am. Chem. Soc.* 109 (1987) 1746.
- [11] Y. Sun, C. LeBlond, J. Wang, D.G. Blackmond, J. Laquidara, J.R. Sowa Jr., *J. Am. Chem. Soc.* 117 (1995) 12647.
- [12] U.K. Singh, M.A. Vannice, *J. Mol. Catal.*, in press.
- [13] C.N. Satterfield, *Mass Transfer in Heterogeneous Catalysis*, Robert E. Krieger Publishing Co., New York, 1970.
- [14] J.J. Carberry, *Chemical and Catalytic Engineering*, McGraw-Hill, New York, 1976.
- [15] R.J. Madon, M. Boudart, *Ind. Eng. Chem. Fundam.* 21 (1982) 438.
- [16] R. Koros, E.J. Nowak, *Chem. Eng. Sci.* 22 (1967) 470.
- [17] F. Notheisz, A. Zsigmond, M. Bartok, Z. Szegletes, G.V. Smith, *Appl. Catal. A: Gen.* 120 (1994) 105.
- [18] U.K. Singh, M.A. Vannice, *J. Catal.*, in press.
- [19] P.B. Weisz, *Z. Phys. Chem.* 11 (1957) 1.
- [20] R. Chambers, M. Boudart, *J. Catal.* 6 (1966) 141.
- [21] E.W. Thiele, *Ind. Eng. Chem.* 31 (1939) 916.
- [22] G.W. Roberts, H.H. Lamb, *J. Catal.* 154 (1995) 364.
- [23] I. Bergault, P. Fouilloux, C. Joly-Vuillemin, H. Delmas, *J. Catal.* 175 (1998) 328.
- [24] S. Topinen, T.-K. Rantakyla, T. Salmi, J. Aittama, *Catal. Today* 38 (1997) 23.
- [25] S. Topinen, T.-K. Rantakyla, T. Salmi, J. Aittama, *Ind. Eng. Chem. Fundam.* 35 (1996) 1824.
- [26] S. Topinen, PhD Thesis, Abo Akademi University, 1996.
- [27] U.K. Singh, R.N. Landau, Y. Sun, C. LeBlond, D.G. Blackmond, S. Tanielyan, R.L. Augustine, *J. Catal.* 154 (1995) 91.
- [28] Y. Sun, J. Wang, C. LeBlond, R.N. Landau, D.G. Blackmond, *J. Catal.* 161 (1996) 759.
- [29] Y. Sun, R.N. Landau, J. Wang, C. LeBlond, D.G. Blackmond, *J. Am. Chem. Soc.* 118 (1996) 1348.
- [30] Y. Sun, J. Wang, C. LeBlond, R.A. Reamer, J. Laquidara, J.R. Sowa Jr., D.G. Blackmond, *J. Organomet. Chem.* 548 (1997) 65.
- [31] H.-U. Blaser, H.-P. Jalett, M. Garland, M. Studer, H. Hhies, A. Wirth-Tijani, *J. Catal.* 173 (1998) 282.
- [32] J. Wang, C. LeBlond, C.F. Orella, Y. Sun, J.S. Bradley, D.G. Blackmond, *Stud. Surf. Sci. Catal.* 108 (1996) 183.
- [33] A. Deimling, B.M. Karandikar, Y.T. Shah, N.L. Carr, *Chem. Eng. J.* 29 (1984) 127.
- [34] M. Zajcew, *Am. Oil Chemists' Soc. J.* 37 (1960) 11.
- [35] F.A. Carey, R.J. Sundberg, *Advanced Organic Chemistry*, Plenum Press, New York, 1990 (Chapter 4).
- [36] L. Gilbert, C.I. Mercier, *Stud. Surf. Sci. Catal.* 78 (1993) 51.
- [37] J.T. Wehrli, A.J. Baiker, *Mol. Catal.* 57 (1989) 245.
- [38] H.-U. Blaser, H.P. Jalett, J. Wiehl, *J. Mol. Catal.* 68 (1991) 215.
- [39] R.L. Augustine, *Adv. Catal.* 25 (1976) 56.
- [40] R.L. Augustine, P. Techasavapak, *J. Mol. Catal.* 87 (1994) 95.
- [41] P.G.J. Koopman, H.M.A. Buurmans, A.P.G. Kieboom, H. Bekkum, *Recl. Trav. Chim. Pays-Bas* 100 (1981) 156.
- [42] J.P. Wauquier, J.C. Jungers, *Bull. Soc. Chim Fr.* 1280 (1957).
- [43] L. Cerveny, V. Ruzicka, *Catal. Rev.-Sci. Eng.* 24 (1982) 503.
- [44] R.A. Rajadhyaksha, S.L. Karwa, *Chem. Eng. Sci.* 41 (1986) 1765.
- [45] N.O. Lemcoff, *J. Catal.* 46 (1997) 356.
- [46] H.S. Lo, M.E. Paulaitis, *AIChE J.* 27 (1981) 842.
- [47] A. Gamez, J. Kohler, J. Bradley, *Catal. Lett.* 55 (1998) 73.
- [48] T. Mallat, Z. Bodnar, B. Minder, K. Borszeczy, A. Baiker, *J. Catal.* 168 (1997) 183.
- [49] J. Struijk, J.J.F. Scholten, *Appl. Catal. A: Gen.* 82 (1992) 277.
- [50] P.J. van der Steen, J.J.F. Scholten, *Appl. Catal.* 58 (1990) 281.
- [51] P.J. van der Steen, J.J.F. Scholten, *Appl. Catal.* 58 (1990) 291.
- [52] J. Struyk, J.J.F. Scholten, *Appl. Catal.* 62 (1990) 151.
- [53] R. West, *J. Am. Chem. Soc.* 81 (1959) 1615.
- [54] E.E. Gonzo, M. Boudart, *J. Catal.* 52 (1978) 462.
- [55] M. Boudart, D.J. Sajkowski, *Faraday Discuss.* 92 (1991) 57.
- [56] R.J. Madon, J.P. O'Connell, M. Boudart, *AIChE J.* 24 (1978) 904.
- [57] J.M. Bronsted, *Z. Phys. Chem.* 102 (1922) 169.
- [58] K.F. Wong, C.A. Eckert, *I&E.C. Proc. Des. Dev.* 8 (1969) 569.
- [59] M. Boudart, G. Djega-Mariadassou, *Kinetics of Heterogeneous Catalytic Reactions*, Princeton University Press, Princeton, NJ, 1984.
- [60] U.K. Singh, M.A. Vannice, *AIChE J.* 5 (1999) 1059.
- [61] L. Cerveny, B. Vostry, V. Ruzicka, *Collect. Czech Chem. Commun.* 46 (1981) 1965.
- [62] J.S. Bradley, W. Busser, *Catal. Lett.* 63 (1999) 127.
- [63] A. Baiker, *Chem. Rev.* 99 (1999) 453.
- [64] D.C. Wynne, M.M. Olmstead, P.G. Jessop, *J. Am. Chem. Soc.* 122 (2000) 7638.

- [65] A. Stanislaus, B. Cooper, *Catal. Rev.-Sci. Eng.* 36 (1994) 75.
- [66] J.P. Boitiaux, J. Cosyns, E. Robert, *Appl. Catal.* 32 (1987) 145.
- [67] J.P. Boitiaux, J. Cosyns, E. Robert, *Appl. Catal.* 32 (1987) 169.
- [68] J.P. Boitiaux, J. Cosyns, E. Robert, *Appl. Catal.* 35 (1987) 193.
- [69] G. Neri, M.G. Musolino, L. Bonaccorsi, A. Donato, L. Mercadante, S. Galvagno, *Ind. Eng. Chem. Res.* 36 (1997) 3619.
- [70] D.E. Gardin, X. Su, P.S. Cremer, G.A. Somorjai, *J. Catal.* 158 (1996) 193.
- [71] J.E. Rekoske, R.D. Cortright, S.A. Goddard, S.B. Sharma, J.A. Dumesic, *J. Phys. Chem.* 96 (1992) 1880.
- [72] J.A. Dumesic, D.F. Rudd, L.M. Aparicio, J.E. Rekoske, A.A. Trevino, *The Microkinetics of Heterogeneous Catalysis*, ACS Professional Reference Book, 1993 (Chapter 5).
- [73] P. Chou, M.A. Vannice, *J. Catal.* 107 (1987) 123.
- [74] S. Lin, M.A. Vannice, *J. Catal.* 143 (1993) 539.
- [75] R. Shekhar, M.A. Barteau, R.V. Plank, J.M. Vohs, *J. Phys. Chem. B* 101 (1997) 7939.
- [76] J.L. Davis, M.A. Barteau, *J. Am. Chem. Soc.* 111 (1989) 1782.
- [77] S. Tsuchiya, Y. Amenomiya, R.J. Cvetanovic, *J. Catal.* 19 (1970) 245.
- [78] V.Y. Konyukhov, A.G. Zyskin, N.V. Kul'kova, M.I. Temkin, *Kinetika i Kataliz* 26 (1985) 1489.
- [79] S. Sato, K. Miyahara, *J. Res. Inst. Catal. Hokkaido Univ.* 22 (1974) 172.
- [80] R.W. McCabe, L.D. Schmidt, *Surf. Sci.* 66 (1977) 101.
- [81] G. Ertl, M. Neumann, K.M. Streit, *Surf. Sci.* 64 (1977) 393.
- [82] M. Englisch, V.S. Ranade, J.A. Lercher, *Appl. Catal. A: Gen.* 163 (1997) 111.
- [83] A. Waghay, D.G. Blackmond, *J. Phys. Chem.* 97 (1993) 6002.
- [84] C.J. Houtman, M.A. Barteau, *J. Catal.* 130 (1991) 528.
- [85] N.F. Brown, M.A. Barteau, *J. Am. Chem. Soc.* 114 (1992) 4258.
- [86] D.E. Mears, M. Boudart, *AIChE J.* 12 (1966) 313.
- [87] M. Boudart, *AIChE J.* 18 (1972) 465.
- [88] M.A. Vannice, S.H. Hyun, B. Kalpakci, W.C. Liauh, *J. Catal.* 56 (1979) 358.
- [89] D. Godbey, F. Zaera, R. Yeates, G.A. Somorjai, *Surf. Sci.* 167 (1986) 150.
- [90] N.M. Abbas, R.J. Madix, *Appl. Surf. Sci.* 7 (1981) 241.
- [91] P. Gallezot, A. Giroir-Fendler, D. Richard, in: W.E. Pascoe (Ed.), *Catalysis of Organic Reactions*, Vol. 47, Chemical Industry, 1992.
- [92] G.L. Haller, D.E. Resasco, *Adv. Catal.* 36 (1989) 173.
- [93] B. Sen, M.A. Vannice, *J. Catal.* 113 (1988) 52.
- [94] B. Sen, M.A. Vannice, *J. Catal.* 115 (1989) 65.
- [95] M.A. Vannice, *Top. Catal.* 4 (1997) 241.
- [96] L. Pauling, *Proc. R. Soc. London, Ser. A* 196 (1949) 343.
- [97] F. Delbecq, P. Sautet, *J. Catal.* 152 (1995) 217.
- [98] Fadley, D.A. Shirley, in: *Proceedings of the 3rd Materials Research Symposium on Electronic Density of States*, Gaithersburg, MD, 3–6 November 1969.
- [99] M. Boudart, *Adv. Catal.* 20 (1969) 153.
- [100] M. Boudart, *Proc. Int. Congr. Catal.* 6 (1976) 11.
- [101] G.C. Bond, *Surf. Sci.* 156 (1985) 966.
- [102] M. Che, C.O. Bennett, *Adv. Catal.* 36 (1989) 55.
- [103] V. Ponec, *Adv. Catal.* 32 (1983) 101, 149.
- [104] C.O. Bennett, M. Che, *J. Catal.* 120 (1989) 293.
- [105] R.I. Masel, *Principles of Adsorption and Reaction on Solid Surfaces*, Wiley, New York, 1996 (Chapter 6).
- [106] G.C. Bond, *Acc Chem. Res.* 26 (1993) 490.
- [107] M. Boudart, *Z. Phys. Chem.* 197 (1996) 21.
- [108] G.A. Somorjai, J. Carrazza, *Ind. Eng. Chem. Fundam.* 25 (1986) 63.
- [109] J.M. Basset, G. Dalmai-Imelik, M. Primet, R. Mutin, *J. Catal.* 37 (1975) 22.
- [110] F. Zaera, G.A. Somorjai, *J. Am. Chem. Soc.* 106 (1984) 2288.
- [111] G.C. Bond, *Appl. Catal. A: Gen.* 149 (1997) 3.
- [112] T.P. Beebe Jr., J.T. Yates Jr., *J. Am. Chem. Soc.* 108 (1986) 663.
- [113] S.J. Thomson, G.J. Webb, *Chem Soc. Chem Commun.* 526 (1976).
- [114] G.A. Somorjai, *Langmuir* 7 (1991) 3176.
- [115] G.A. Somorjai, *J. Mol. Catal. A: Chem.* 107 (1996) 39.
- [116] G. Dalmai-Imelik, J. Massardier, in: G.C. Bond, P.B. Wells, F.C. Tompkins (Eds.), *Proceedings of the 6th International Congress on Catalysis*, Vol. 1, London, 1976, The Chemical Society, 1977, p. 90.
- [117] W.H. Manogue, J.R. Katzer, *J. Catal.* 32 (1974) 166.
- [118] U.K. Singh, M.A. Vannice, in: *Proceedings of the 12th International Congress on Catalysis*, Stud. Surf. Sci. Catal., A. Korma et al. (Eds.) 130 (2000) 497.
- [119] R. van Hardeveld, F. Hartog, *Surf. Sci.* 15 (1969) 189.
- [120] J. Oudar, *Z. Phys. Chem.* 197 (1996) 125.
- [121] T. Birchem, C.M. Pradier, Y. Berthier, G. Cordier, *J. Catal.* 146 (1994) 503.
- [122] C.M. Pradier, T. Birchem, Y. Berthier, G. Cordier, *Catal. Lett.* 29 (1994) 371.
- [123] T. Birchem, C.M. Pradier, Y. Berthier, G. Cordier, *J. Catal.* 161 (1996) 68.
- [124] L.P. Ford, H.L. Nigg, P. Blowers, R.I. Masel, *J. Catal.* 179 (1998) 163.
- [125] L. Mercadante, G. Neri, C. Milone, A. Donato, S. Galvagno, *J. Mol. Catal. A: Chem.* 105 (1996) 93.
- [126] M. Englisch, A. Jentys, J.A. Lercher, *J. Catal.* 166 (1997) 25.
- [127] A. Giroir-Fendler, D. Richard, P. Gallezot, *Catal. Lett.* 5 (1990) 175.
- [128] S. Galvagno, G. Capannelli, G. Neri, A. Donato, R. Pietropaolo, *J. Mol. Catal.* 64 (1991) 237.
- [129] P. Beccat, J.C. Bertolini, Y. Gauthier, J. Massardier, P. Ruiz, *J. Catal.* 126 (1990) 451.
- [130] T.B.L.W. Marinelli, S. Nabuurs, V. Ponec, *J. Catal.* 151 (1995) 431.
- [131] J.C. Jesus, F. Zaera, *Surf. Sci.* 430 (1999) 99.